ESSOAr | https://doi.org/10.1002/essoar.10507536.1 | CC_BY_4.0 | This content has not been peer reviewed.

A hydrochemically guided landscape-based classification for water quality: a case study application of process-attribute mapping (PoAM) at a national scale

Clinton W.F. Rissmann[1,2], Lisa K. Pearson[1], Adam P. Martin[3], Matthew I. Leybourne[4], W. Troy Baisden[5], Timothy J. Clough[6], Richard W. McDowell[7], and Jenny G. Webster-Brown[7]

[1] Land and Water Science, 90 Layard Street, Invercargill 9810, New Zealand.

[2] Waterways Centre for Freshwater Management, University of Canterbury and Lincoln University, Private Bag 4800, Christchurch 8140, New Zealand.

[3] GNS Science, Private Bag 1930, Dunedin 9054, New Zealand.

[4] Queen's Facility for Isotope Research, Department of Geological Sciences and Geological Engineering, and Arthur B. McDonald Canadian Astroparticle Physics Research Institute, Department of Physics, Engineering Physics & Astronomy, Queens University, Kingston, Ontario, Canada.

[5] University of Waikato, Private Bag 3105, Hamilton 3240, New Zealand.

[6] Lincoln University, PO Box 85084, Lincoln 7647, New Zealand.

[7] National Science Challenge, AgResearch, Lincoln Science Centre, Private Bag 4749, Christchurch 8140, New Zealand.

Corresponding author: Clinton Rissmann (clint@landwatersci.net)

OICID
Clinton Rissmann 0000-0002-1550-5365
Lisa Pearson 0000-0002-0746-871X
Adam Martin 0000-0002-4676-8344
Matthew Leybourne 0000-0002-2361-6014
Troy Baisden 0000-0003-1814-1306
Tim Clough 0000-0002-5978-5274
Richard McDowell 0000-0003-3911-4825
Jenny Webster Brown 0000-0001-9665-871X

Key Points:

- A few dominant processes (atmospheric, hydrological, redox, chemical and physical weathering) govern spatial variability in water quality
- Hydrochemistry is used to guide the mapping of dominant process-gradients and expert knowledge and machine learning is used to validate
- Failure to consider dominant process-gradients in modeling and policy application risks poor water quality outcomes

ESSOAr | https://doi.org/10.1002/essoar.10507536.1 | CC_BY_4.0 | This content has not been peer reviewed.

Abstract

Spatial variation in landscape attributes can account for much of the variability in water quality compared to land use factors. Spatial variability arises from gradients in topographic, edaphic, and geologic landscape attributes that govern the four dominant processes (atmospheric, hydrological, microbially mediated redox, physical and chemical weathering) that generate, store, attenuate, and transport contaminants. This manuscript extends the application of Process Attribute Mapping (PoAM), a hydrochemically guided landscape classification system for modelling spatial variation in multiple water quality indices, using New Zealand (268,021 km²) as an example. Twelve geospatial datasets and >10,000 ground and surface water samples from 2,921 monitoring sites guided the development of 16 process-attribute gradients (PAG) within a geographic information system. Hydrochemical tracers were used to test the ability of PAG to replicate each dominant process (cross validated R^2 of 0.96 to 0.54). For water quality, land use intensity was incorporated and the performance of PAG was evaluated using an independent dataset of 811 long-term surface water quality monitoring sites (R^2 values for total nitrogen of 0.90 - 0.71 (median = 0.78), nitrate-nitrite nitrogen 0.83 - 0.71 (0.79), total phosphorus 0.85 - 0.63 (0.73), dissolved reactive phosphorus 0.76 - 0.57 (0.73), turbidity 0.92 - 0.48 (0.69), clarity 0.89 - 0.50 (0.62) and *E. coli* 0.75 - 0.59 (0.74)). The PAGs retain significant regional variation, with relative sensitivities related to variable geological and climatic histories. Numerical models or policies that do not consider landscape variation likely produce outputs or rule frameworks that may not support improved water quality.

Plain Language Summary

In the wrong place, or at excessive concentrations, nutrients (nitrogen and phosphorus) and sediment become contaminants. Along with pathogens (harmful microbes), they require reduction to improve water quality globally. Landscape variation can result in significant differences in water quality despite similar land use pressures. Landscape variation been mapped for New Zealand using a novel landscape classification system, termed Process Attribute Mapping to explain how and why water quality varies spatially. The classification uses twelve pre-existing map datasets and >10,000 ground and surface water samples from 2,921 monitoring sites to depict differences as national process attribute gradient (PAG) maps. Each PAG was tested against tracers (such as chloride, iron, and calcium) measured in surface water samples. The ability of PAG to represent steady-state water quality, as indicated by nitrogen, phosphorus, sediment, and a microbial indicator, was assessed by combining an independent dataset of 811 long-term surface water quality monitoring sites and a map representing the gradient in land use intensity. The modelling identified regional climatic and geological variation as key controls on water quality variation across New Zealand. The PAG will now be combined into a single national classification for water quality. This methodology should be applicable globally.

ESSOAr | https://doi.org/10.1002/essoar.10507536.1 | CC_BY_4.0 | This content has not been peer reviewed.

1 Introduction

Water quality, as indicated by concentrations of nitrogen and phosphorus species, organic and inorganic sediment, and the faecal indicator bacterium *Escherichia coli* (*E. coli)*, can vary spatially across a landscape, even when land use is spatially uniform. These water quality differences occur because of natural spatial variation in several processes (atmospheric, hydrological, microbially mediated redox, physical and chemical weathering) that determine the composition of water (Moldan and Černý, 1994; Clark and Fritz, 1997, Drever and Stillings, 1997; Kendall and McDonnell, 1998; Güler et al., 2002; McMahon and Chapelle, 2008; Tratnyek et al., 2012; Daughney et al. 2015). These processes are also coupled to gradients in landscape attributes, such as topography and geology.

Gradients in the volume and intensity of precipitation, an atmospheric *process*, are primarily driven by weather patterns and local scale topographic variation (landscape *attribute*) (Clark and Fritz, 1997; Drever and Stillings, 1997; Kendall and McDonnell, 1998). The hydrological process is driven by climate, catchment topography, edaphic and geological attributes (Clark and Fritz, 1997; Kendall and McDonnell, 1998; James and Roulet, 2006; Inamdar, 2011). Groundwater redox depends on the abundance of electron donors within an aquifer (Drever and Stillings, 1997; Krantz and Powars, 2000; McMahon and Chapelle, 2008). Mass weathering processes are determined by bedrock characteristics (Mueller and Pitlick, 2013). The pH, ionic composition, and alkalinity of surface and ground waters is strongly influenced by the acid neutralising capacity of soil and rock (Wright, 1988; Drever and Stillings, 1997; Leybourne and Goodfellow, 2010). These and other component processes may account for the majority of water quality variation, compared to land use on its own, through regulating the generation, storage, attenuation, and transport of contaminants in the environment (Johnson et al., 1997; Hale et al., 2004; King et al., 2005; Dow et al., 2006; Shiels, 2010; Becker et al., 2014). Accordingly, the role that landscape plays in determining water quality variation is critically important, and especially so for geologically diverse settings, such as New Zealand (Johnson et al., 1997).

Given the importance of landscape attributes, many ‘controlling landscape factor' classifications have been developed to generate landscape or riverine classes that discriminate variation in water quality. Such classification schemes include: 1) the United States Environmental Protection Agency's and the United States Geological Survey's Ecoregion and Ecological land approaches, which have been applied globally (Dinerstein et al., 2017; Omernik and Griffith, 2014; Sayre et al., 2014); 2) the European Water Framework Directive's Ecoregions (Hughes and Larsen, 1988; European Commission, 2000); and 3) the River Environment Classification, which has been applied across New Zealand (Snelder et al., 2005). These landscape classification schemes typically employ a top-down approach that groups landscape attributes into classes according to similar climatic, topographic, edaphic, or geologic attributes, and these have been used to discriminate variation in a wide range of characteristics, including hydrology, water quality and ecological characteristics.

In the work presented here, hydrochemical knowledge, in conjunction with measures of process-specific tracers in surface and shallow groundwaters, is used to guide the identification, organisation, and subsequent classification of landscape attributes that govern gradients in each dominant process. The focus on mapping dominant processes gradients and the use of hydrochemical tracers to guide the classification of the landscape differs from traditional landscape factor classification methods (Hughes and Larsen, 1988; Omernik and Griffith, 2014;

ESSOAr | https://doi.org/10.1002/essoar.10507536.1 | CC_BY_4.0 | This content has not been peer reviewed.

Sayre et al., 2014; Dinerstein et al., 2017). Surface and groundwater chemistry is a valuable tool for reconstructing the origins and history of water (Clark and Fritz, 1997; Drever, 1997; Kendall and McDonnell, 1998). Analysing hydrochemical tracers, for a given process, within surface waters and shallow unconfined aquifers also provides a process-level reference or control point. This permits relationships between processes and landscape attributes to be evaluated and hypotheses regarding such relationships to be refined. Thus, hydrochemistry is useful for guiding the production of a more representative classification than is possible through a purely top-down approach.

In addition to the established understanding of the relationship between process gradients and landscape attributes provided by hydrochemistry, we also hypothesise that a small number of dominant processes govern spatial variation in water quality. This hypothesis follows Grayson and Blöschl's (2001) dominant process concept, which suggests that the response of environmental systems is generally explained by a small number of dominant processes. Grayson and Blöschl (2001) also proposed that a logical way to identify the dominant processes is by evaluating the sensitivity of the system to each of the individual processes (believed to have influence) through a (high-order) multi-variable sensitivity analysis and selecting those variables with significant influence (Sivakumar, 2004; 2008).

This manuscript describes the application and testing of a hydrochemically guided landscape classification system specifically for water quality. The method, developed originally for Southland, New Zealand, is termed Process-Attribute Mapping (PoAM) (Rissmann et al., 2019). PoAM applies a practical hydrochemical method, at a macroscale, to generate spatial representations of the four dominant processes that determine spatial variation in water quality: this generates a series of graphical outputs, or maps. Each graphical output is referred to as a 'process-attribute gradient' that represents, at a macroscale, the coupling between a dominant process (or component process) and its controlling landscape attributes.

2 Materials and Methods

2.1 High level overview of PoAM method

The PoAM conceptual framework and model presented here was developed from Rissmann et al. (2018a, 2019; **Fig. 1**) and a step-by-step description of the PoAM method is provided in the supporting information **S1**. Two examples of process-attribute gradient development are also provided to support the readers understanding of the method (**S2 and S3**). Further, examples of the use of hydrochemical and water quality data to generate process-attribute gradients are provided by Rissmann et al. (2016a, 2018a, b, 2019). The PoAM method results in a depiction of the landscape, at a macroscale, showing zones within the landscape at a level where dominant process occur (e.g., redox, not denitrification). Through mapping each dominant process gradient instead of an individual contaminant (e.g., nitrate only), reaction process (e.g., denitrification only), or hydrological pathway (e.g., vertical percolation through the soil matrix to an underlying aquifer only), PoAM produces macroscale, landscape classifications capable of providing process-level context. For example, 'why' is nitrate concentration elevated in one stream but not another?

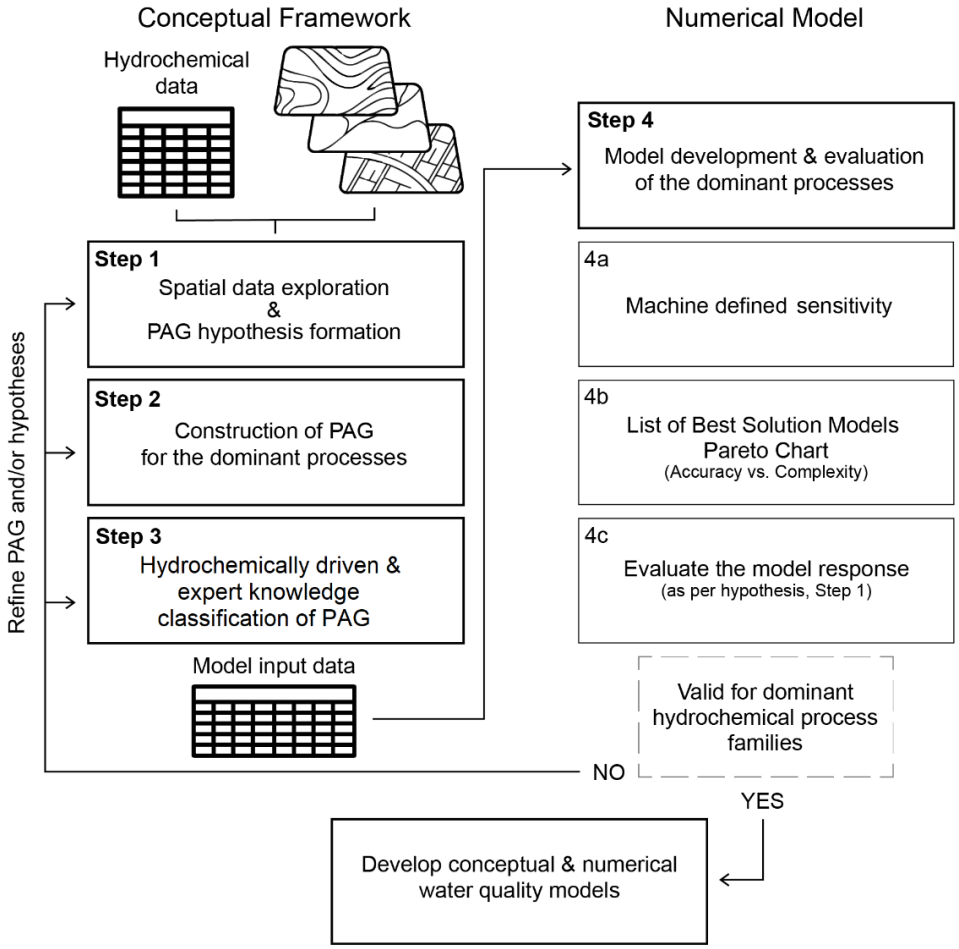

Figure 1. A flow chart summary of key steps in process-attribute mapping (PoAM) (adapted from Rissmann et al., 2019; see **S1**). The conceptual model provides a spatial representation of the key processes and contaminant transport pathways whilst the numerical models provide an estimate of steady-state median surface water concentration. PAG: process-attribute gradient.

PoAM utilises existing geospatial classifications of climate, topography, soil, geology and hydrochemical data to build graphical representations of each process-attribute within a geographic information system (GIS). During the development of process-attribute gradients, hydrochemical data is used to:

i. refine hypotheses about controlling landscape factors through evaluating the relationship between hydrochemical process signals and landscape attributes;
ii. support the identification and combination of relevant landscape attributes from pre-existing geospatial datasets to generate process-attribute gradients; and
iii. drive the grouping of landscape attributes into classes.

Following process-attribute gradient development, a series of high-level hypotheses are proposed about the likely sensitivity and magnitude of response (i.e., increase or decrease in concentration) of each hydrochemical tracer(s) for each dominant process. Each hypothesis is tested using the hybrid deterministic genetic programming (HDGP) approach of Schmidt and Lipton (2015). The HDGP method is specifically designed to reveal the underlying relationships

between a target variable (i.e., hydrochemical tracer) and one or more predictors (i.e., process-attribute gradients). The method employs symbolism (white box), is unsupervised and evolutionary, discarding any process-attribute gradients that do not reduce the modelled relationships uncertainty and complexity (Khu et al., 2001; Schmidt and Lipson, 2009, 2015; Rissmann et al., 2019). The machine defined sensitivities and magnitude of response for each tracer are compared with the hypothesised response derived from expert knowledge of the process level controls (**Fig. 1**; Rissmann et al., 2019). If the machine defined response is consistent with the hypothesis for each hydrochemical tracer and the modelled relationships are reasonable, i.e., cross-validated $R^2 > 0.65$, they are considered to provide a representation of the actual process-attribute gradient. Only then are process-attribute gradients deemed fit to be combined with a representation of land-use pressure and development of water quality models. If a region is characterised by a distinct geological feature (e.g., geothermal activity), or climatic history (e.g., no history of glaciation), deviation from the high-level hypotheses is expected.

In practice, the multivariate testing of process-attribute gradients requires surface water capture zones to be generated for each surface water hydrochemical site (n = 730 nationally) and mean scores for each process-attribute gradient to be calculated. Median hydrochemical concentrations and mean process-attribute scores are then spatially joined in a tabular format and used as the input for multivariate assessment (**Fig. 1**). Following multivariate testing of the hydrochemical tracers of each dominant process, a representation of land use pressure (i.e., intensity) is incorporated and process-attribute gradients are used to evaluate spatial variation in median total nitrogen, nitrate-nitrite nitrogen, total phosphorus, dissolved reactive phosphorus, *E. coli*, clarity (black disk), and turbidity (Nephelometric turbidity units) across 811 long-term surface water quality monitoring sites nationally.

2.2 Case study setting

New Zealand is characterised by a diversity of topography, climate, soil type, geology, and land cover. The New Zealand climate varies from subtropical in the north to cool temperate in the south, with cold (< 0 °C mean annual temperature) alpine conditions in the mountainous areas. Rainfall is typically between 300 and 1600 mm per annum, although this can exceed 9000 mm across alpine regions of the South Island. Relief is up to 3724 m along the north-northeast trending Southern Alps mountain chain that bisects the South Island (**Fig. 2**), and isolated volcanic centres are up to 2797 m-high on the North Island. Andosols and Cambisols (United Nations, Food and Agricultural Organisation Soil Classification) are the dominant soil types, with multiple other soil types present, including Podzols, Luvisols, Gleysols, Arenosols, Acrisols, Panosols, Phaeozems and Nitisols (de Sousa et al., 2020). The geology of New Zealand is divided into a variety of volcanic, intrusive and sedimentary terranes that make up the basement rocks of the Austral Superprovince, and the overlying, mainly sedimentary and volcanic rocks of the Zealandia Megasequence, are separated from basement by a diachronous regional unconformity between 117 and 105 Ma (Edbrooke et al., 2015). Land cover (updated 2018) is dominated by pasture (c. 40 %), indigenous forests (c. 26 %), cropland, exotic forest and urban areas. New Zealand has > 70 major river systems and c. 425 000 km-length of rivers and streams, with 51 % in catchments dominated by native vegetation and the rest in modified landscapes (Ministry for the Environment and Stats NZ, 2020). High temperature (> 180 °C) volcanic-hydrothermal activity is mainly restricted to the Taupo Volcanic Zone (**Fig. 2**).

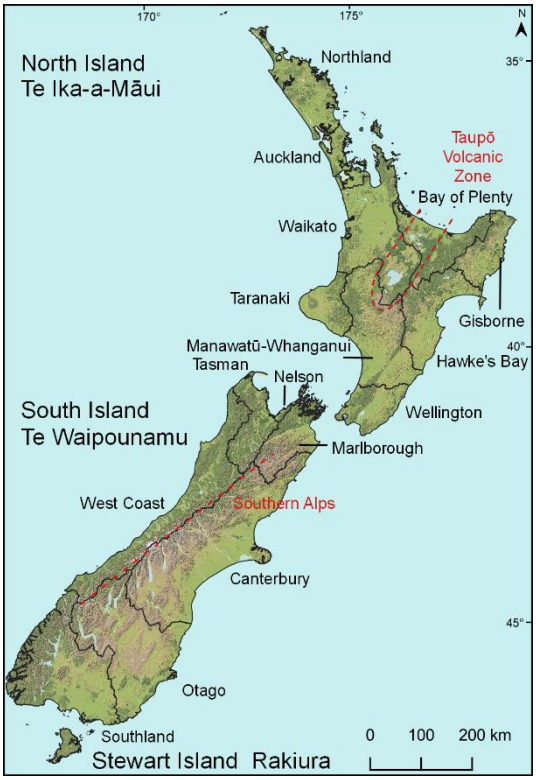

Figure 2. Map of New Zealand subdivided by region. Also shown is the trace of the Southern Alps mountain chain and the location of the Taupo Volcanic Zone. Base layer is realistic land cover from Geographx (2009).

3 Data

3.1 Hydrochemical and water quality datasets

Chemical analyses of low, median, and event flows were taken from 730 long-term surface water monitoring sites across the regions of Northland, Auckland, Waikato, Bay of Plenty, Manawatū-Whanganui, Canterbury, and Southland (58 % of New Zealand), between 2017 and 2019 (**Table 1** and **Fig. 3**). Across the same regions and for the same time period, data for the sample chemical constituents were collected at 2,191 long-term groundwater monitoring sites (**Table 1**). The respective hydrochemical datasets for surface water and groundwater were subsequently combined with pre-existing hydrochemical data collected between 2007-2017 and median concentrations calculated (Pearson and Rissmann, 2021a). Detailed information of the sampling methodologies, field measures, laboratory analysis, calculation of hydrochemical metrics (e.g., major ion facies, saturation indices) and quality assurance and quality control of the samples used in this project are provided in Rissmann et al. (2016).

Table 1. Hydrochemical and water quality analyses used in this study.

Dataset	Type	Analyte	Units	Parameter Name
Hydrochemical (surface water and groundwater)	Major Constituents	Ca	mg/L	Dissolved calcium [1]
		Cl	mg/L	Dissolved chloride
		DOC	mg/L	Dissolved organic carbon
		HCO_3	mg $CaCO_3$/L	Dissolved bicarbonate alkalinity [2]
		K	mg/L	Dissolved potassium
		Mg	mg/L	Dissolved magnesium
		Na	mg/L	Dissolved sodium
		SO_4	mg/L	Dissolved sulphate
		SiO_2	mg/L	Dissolved reactive silica
	Minor Constituents	B	mg/L	Dissolved boron
		Br	mg/L	Dissolved bromide
		F	mg/L	Dissolved fluoride
		Fe	mg/L	Dissolved iron
		I	mg/L	Dissolved iodide
		Mn	mg/L	Dissolved manganese
	Field Parameters	Clarity	m	Visual clarity
		DOField	mg/L	Dissolved oxygen (field measured)
		EC	µS/cm	Electrical conductivity [3], temperature corrected
		ORP	mV	Oxidation-reduction potential
		pHField	pH units	pH (field measured)
		pHLab	pH units	pH (lab measured)
		Temp	°C	Water Temperature
Water quality (surface water)	Nutrients	TN	mg N/L	Total nitrogen
		NNN	mg N/L	Nitrate nitrite nitrogen
		TP	mg P/L	Total phosphorus
		DRP	mg P/L	Dissolved reactive phosphorus
	Suspended Sediment	Black disk	m	Visual clarity
		Turb	NTU[4]	Turbidity
	Biological	*E. coli*	cfu/100 mL	Escherichia coli

[1] Most samples were filtered (0.45 µm) prior to analysis, and therefore analytical results reflect "dissolved" rather than total concentrations. However, it is noted that many colloidal species will pass through a 0.45 µm filter.

[2] The United States Geological Survey notes that alkalinity is not a chemical in water, but, rather, it is a property of water that is dependent on the presence of bicarbonates, carbonates, and hydroxides. As such, alkalinity is defined as a measure of the ability of the water body to neutralize acids and bases and thus maintain a fairly stable pH level.

[3] Microsiemens per centimeter.

[4] Nephelometric turbidity units.

An independent surface water quality dataset comprising 991 long-term monitoring sites across New Zealand was downloaded from Land Air Water Aotearoa (LAWA) for 2014 – 2018 (**Table 1** and **Fig. 3a**). This dataset was collected by each regional authority, with quality assurance performed according to National Environmental Monitoring and Reporting Standards (Davies-Colley et al., 2012). A minimum of 60 repeat measures are included for each site. Internal quality control in this project removed urban catchments and sites with point source impacts, including sites downstream of municipal wastewater discharges, reducing the dataset to 811 sites. Site water quality medians were calculated for each monitoring point (Pearson and Rissmann, 2021b). No water quality measures from the 811 long-term monitoring sites were used in the generation of process-attribute gradients.

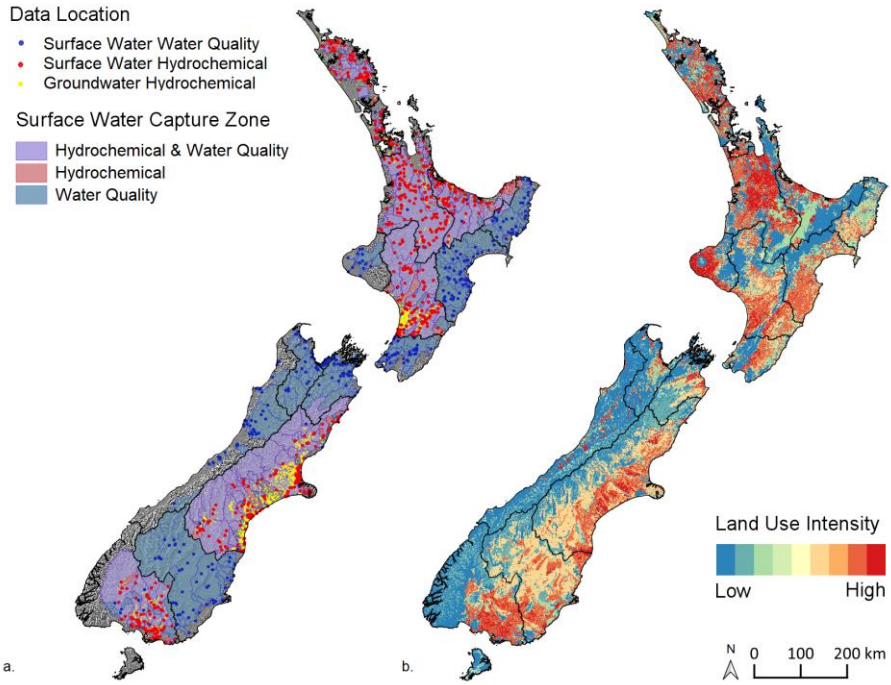

Figure 3. a) Surface and ground water sample locations for hydrochemical (Table 1) and water quality data sets (Table 2 – a minimum of 60 repeat samples for each site) used in PoAM; and b) A map of the land use intensity gradient across New Zealand. The regional boundaries are shown by black outlines.

3.2 Geospatial datasets

For the national application of PoAM, attributes were selected from several national and one regional GIS datasets. This included: 1) topography, elevation and altitude from an 8 m digital elevation model (Land Information New Zealand, 2012); 2) geological attributes from the 1:250 000 geological map series (QMAP, Heron, 2014) and the New Zealand Land Resource Inventory (NZLRI; 1:50 000; Manaaki Whenua Landcare Research, 2000a,b; Newsome et al., 2008; Lynn et al. 2009); 3) soil attributes from SMap (1:50 000, Manaaki Whenua Landcare Research, 2019a) and Fundamental Soils Layer (1:50 000; Manaaki Whenua Landcare Research, 2000c); 4) land cover from the Land Cover Database (LCDBv5; Manaaki Whenua Landcare Research, 2019b); and 5) land use from Land Use Mapping Report (LUCASv006; Ministry for the Environment, 2019). For hydrological input data: 1) river lines, stream Strahler order and catchment areas (capture zones) were sourced from the River Environment Classification (v 2.4; Snelder and Biggs, 2002); 2) precipitation volume was derived from the National Climate Database (Ministry for the Environment, 2016); 3) $\delta^{18}O\text{-}H_2O$ of precipitation came from the national isoscape model of Baisden et al. (2016); 4) water table depth is from Westerhoff et al. (2018); and 5) geothermal extent is from Bibby et al. (1995) for the Taupo Volcanic Zone (**Fig. 2**).

Land use intensity and land use for microbial contaminants were derived by combining the Land Use Capability classification of Lynn et al. (2009), LCDBv5 land cover (Manaaki Whenua Landcare Research, 2019b) and LUCAS land use (Ministry for the Environment, 2019) and ranking land use intensity from 1ow to high using expert judgement (**Fig. 3b**).

ESSOAr | https://doi.org/10.1002/essoar.10507536.1 | CC_BY_4.0 | This content has not been peer reviewed.

3.3 Process-attribute gradient generation

After quality assurance, hydrochemical and geospatial datasets were used to generate 16 national-scale process-attribute gradients depicting the four dominant processes (**Tables 2**, **Fig. 1**). A high-level summary of the hypotheses and process-attribute gradients are included in **Supporting Information 1**. Examples of the assessment and development of the precipitation source $\delta^{18}O\text{-}H_2O$ (V-SMOW) and geological reduction potential process-attribute gradients are provided in **Supporting Information 2** and **3**, with further detail of the process-attribute gradients developed provided in Pearson (2015a, b) and Rissmann et al. (2016a, 2018a).

During process-attribute gradient development, a series of high-level hypotheses were developed linking the likely sensitivity and magnitude of the response of individual process-attribute gradients to one or more tracers of each dominant process (see **S1**). For example, based on observed relationships between process signals in water and landscape attributes, a hypothesis was formulated that the conservative tracers of water source, e.g., Cl and Br, will exhibit a positive magnitude (concentration increases) across the macroscale recharge domain from (lowest) Alpine to Hill to Lowland (highest). This hypothesis is consistent with the role of altitude and distance from the coast over the rainout of marine aerosols, an orographic atmospheric process (Clark and Fritz, 1997; Nichol et al., 1997; Rissmann et al., 2016a; see **S1** and **S2**). Hypothesis development included recognising that two or more dominant processes and multiple process-attribute gradients may be required to adequately explain the spatial distribution of one or more hydrochemical tracers across the surface water network (Rissmann et al., 2019). If a region is characterised by a distinct geological (e.g., geothermal activity), or climatic history (e.g., no history of glaciation), variation in the process-attribute gradients retained is expected.

When used for generating water quality models, overland flow, soil slaking and dispersion process-attribute gradients were normalised by the area of developed land (i.e., non-native land cover). This normalization is based on evidence of contaminant source limitation, i.e., low/no anthropogenic contaminant loads, across large areas of undeveloped hill and high country where overland flow is highest, in contrast to developed land with similar topography. The normalisation of these two process-attribute gradients within water quality model development defines a process response resulting in a negative magnitude for most water quality measures, or a sink, for undeveloped land and positive magnitude of these measures for developed land.

A regional-scale geothermal process-attribute gradient was also developed using the apparent resistivity (log of apparent resistivity Ωm) model of Bibby et al. (1995); there is evidence for diffuse geothermal inputs, from high enthalpy (≥ 180 °C) volcanic-hydrothermal systems, influencing hydrochemical composition and water quality of the Bay of Plenty and Waikato regions.

Table 2. Summary of the 16 national-scale process-attribute gradients. Relevant datasets and their scale are also shown.

Process	PAG	Process attribute gradient	Relevant datasets and scales	Attributes
Atmospheric	O18	Precipitation source	8 m DEM, $\delta^{18}O$-H_2O precipitation isoscape (4 km^2 pixel)	$\delta^{18}O$-H_2O, altitude, distance from the coast
	PPT	Precipitation volume	Annual average rainfall (5 km^2 pixel)	Precipitation volume
Hydrological	RCD	Macroscale recharge domain	Soil surveys (1:50,000), Aquifer type and extent (1:50,000)	Altitude, temperature isotherm, river network, Typic Udifluvent (Fluvial Recent) soils
	OLF	Overland flow	Soil surveys (1:50,000), 8 m DEM	Soil texture, drainage class, permeability, slope, area of developed land
	DD	Deep drainage	Soil surveys (1:50,000)	Drainage class, permeability, depth to slowly permeable horizon
	LAT	Lateral drainage	Soil surveys (1:50,000)	Drainage class, permeability, depth to slowly permeable horizon,
	ART	Artificial drainage	Soil surveys, 8 m DEM, Land Cover (1 ha)	Drainage class, permeability, depth to slowly permeable horizon, slope, agricultural land cover
	HYD	Soil slaking and dispersion as a soil hydrological index	Soil surveys (1:50,000)	Soil texture, drainage class, permeability, area of developed land
	NBP	Soil zone bypass	Soil surveys (1:50,000)	Cation exchange capacity, pH
	EWT	Equilibrium water table and aquifer potential	Water Table Model (0.04 km^2 pixel)	Modelled water table depth
Redox	SRP	Soil reduction potential	Soil surveys (1:50,000); soil chemistry profile points.	Drainage class, carbon content
	GRP	Geological aquifer reduction potential	Geological surveys (1:50,000 - 1:250,000)	Rock type (main and sub rocks)
Weathering	SANC	Soil acid neutralization capacity	Soil surveys (1:50,000); geochemical baseline survey (8 km^2)	Soil pH, cation exchange capacity
	GANC	Geological acid neutralization capacity	Geological surveys (1:50,000 - 1:250,000); geochemical baseline survey (8 km^2)	Rock type
	SGC	Surface/top regolith strength	Geological surveys (1:50,000 - 1:250,000)	Rock type and strength
	BGC	Basal regolith strength	Geological surveys (1:50,000 - 1:250,000)	Rock type and strength
Geothermal	GTH	High enthalpy geothermal (≥180 °C)	Log of resistivity (limited to extent of Taupo Volcanic Zone, Fig.1)	Resistivity

PAG: process attribute-gradient; DEM: digital elevation model

4 Multivariate Assessment

4.1 Pre-processing of data

Following process-attribute gradient production, mean surface water capture zone process-attribute scores were calculated for the 730 regional hydrochemical and 811 national water quality monitoring sites (**Fig. 1**). Mean land use intensity scores and capture zone area (ha) were calculated for each capture zone. Mean capture zone scores were joined with the hydrochemical and 5-year water quality datasets. A constant was added to all numeric data to remove 0 or negative values, and the dataset log10 transformed prior to multivariate assessment.

4.2 Hypotheses testing and evaluation of the representativeness of process-attribute gradients

Multivariate testing was first applied to the hydrochemical dataset (**Step 4, Fig. 1;** see **S1**). In this analysis, tracers of each dominant process are the target variables, and process-attribute gradients the predictors. The multivariate assessment provides an independent test of

ESSOAr | https://doi.org/10.1002/essoar.10507536.1 | CC_BY_4.0 | This content has not been peer reviewed.

the sensitivity (importance) and magnitude of response (increase or decrease in concentration) of process-attribute gradients relative to specific hydrochemical tracers of each dominant process (i.e., atmospheric, hydrological, redox, and weathering). This step is important for evaluating the validity of the high-level hypotheses generated during process-attribute gradient development (see **Table S1.1 and S1.2**). For example, the performance of the process-attribute gradients in replicating water source and hydrological connectivity is evaluated against the conservative hydrological tracers Cl and Br; the representativeness of the redox process-attribute gradients is evaluated against FeII and dissolved organic carbon (DOC), and so on. The hydrochemical tracers are chosen based on their relevance as an indicator for a given process. Tracers that have a significant land use origin, e.g., nitrogen, phosphorus or *E.coli* are not used to test process-attribute gradients. For example, dissolved FeII, not total, is used as a redox tracer because of its role as a terminal electron acceptor during microbially mediated redox succession. Iron is also the 5th most abundant element in Earth's crust so is rarely source-limited (Hem, 1985). However, evaluating physical weathering process-attribute gradients is limited by the lack of suitable geochemical tracers, with simple proxies such as clarity and turbidity, a poor substitute for multi-element or isotope proxies of sediment source. Testing of process-attribute gradients was undertaken on the combined data set for the seven regions and repeated with focus on regional subsets due to evidence for geographically independent process level controls over water quality (e.g., geothermal activity).

4.3 Water quality models

Given the evidence for geographically independent process-level controls (e.g., geothermal activity), water quality models were run as regional subsets characterised by similar climatic and geological histories.

5 Results

5.1 Process-attribute gradients

Sixteen process-attribute gradients defining the dominant processes governing hydrochemistry were produced nationally (**Fig. 4, S2 and S3**). Of the 16 process-attribute gradients, two are associated with atmospheric drivers prior to the routing of water by the hydrological network and are macroscale; precipitation volume (**Fig 4a**) and $\delta^{18}O\text{-}H_2O$ of precipitation (V-SMOW; see **S2**). Eight process-attribute gradients are associated with the hydrological drivers of spatial variation in hydrochemistry. Of these, the recharge domain and hydrological connectivity layer are macroscale (**Fig. 4b**). The remaining seven hydrological process-attribute gradients are all associated with the soil zone and represent mesoscale hydrological gradients in percent precipitation occurring as overland flow, deep drainage through the soil profile, lateral drainage, artificial drainage of the soil profile, soil slaking and dispersion, shrink-swell mediated soil zone bypass (**Fig 4c-h**) and water table depth and aquifer potential (see **S3**). The two redox (**Fig 4i, S3**) and both chemical and physical weathering processes (5 process-attribute gradients) are comprised of separate soil and geological process-attribute gradients (**Fig. 4j-n**). Soil process-attribute gradients overlie geological process-attribute gradients, except where bedrock outcrops (Rissmann et al., 2019). Across lowland areas, the geological process-attribute gradients represent the upper portion of the unconfined aquifer system (Rissmann et al., 2019). The regional-scale geothermal process-attribute gradient represents high enthalpy (≥ 180 °C) diffuse volcanic-hydrothermal inputs over the

hydrochemistry and water quality (i.e., ammoniacal N and P) of shallow ground and surface water across the Taupo Volcanic Zone (**Fig. 4o**). Combined, these layers provide the user with a conceptual, macroscale understanding of the landscape factors known to influence water quality across New Zealand.

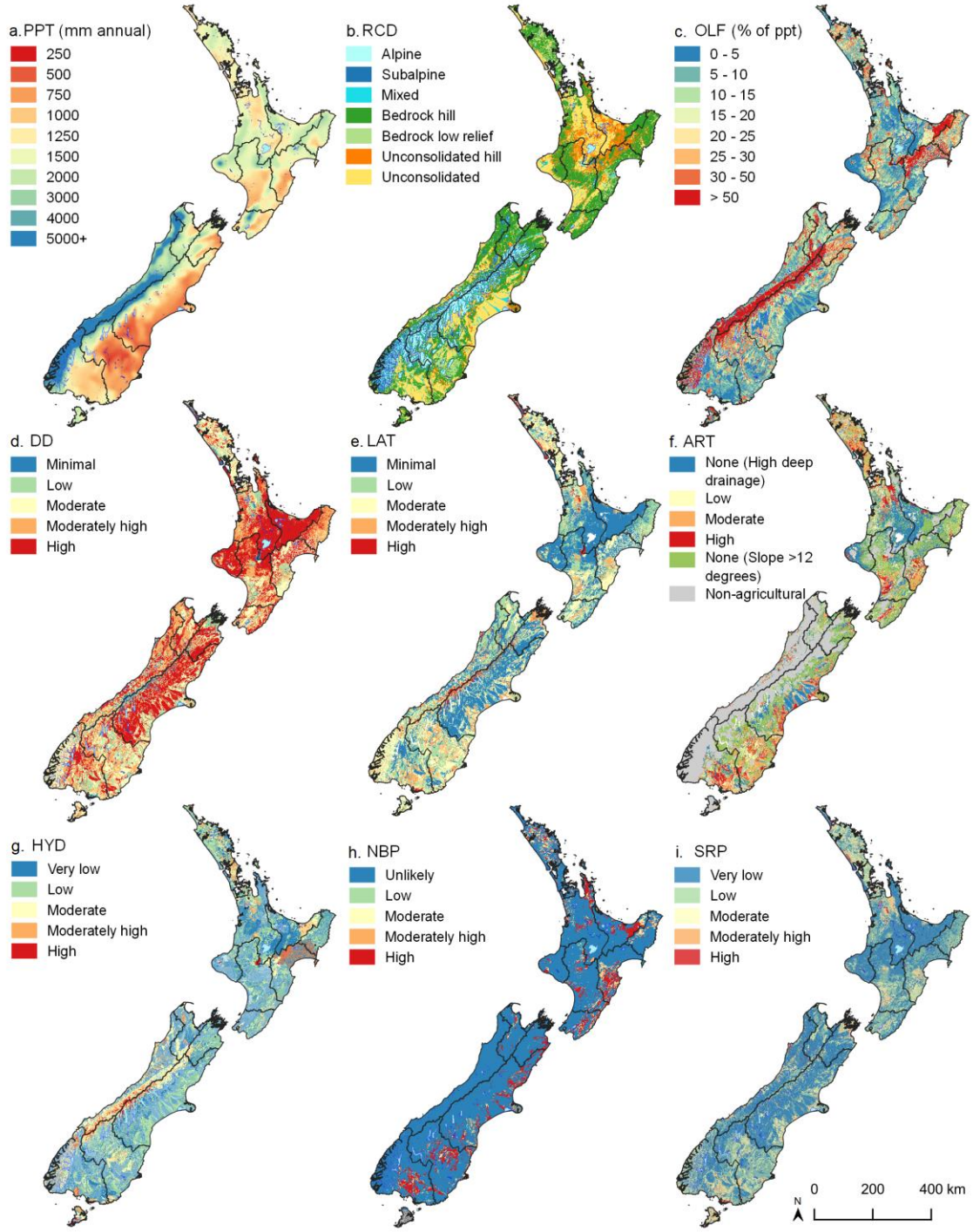

Figure 4. Examples of process attribute gradients representing the 4 dominant processes. a) atmospheric process showing precipitation volume, b) hydrological process showing recharge domain, c) overland flow, d) deep drainage, e) lateral drainage, f) artificial drainage, g) soil

hydrological index of slaking and dispersion, h) natural soil zone bypass under soil moisture deficit, i) redox process showing soil reduction potential.

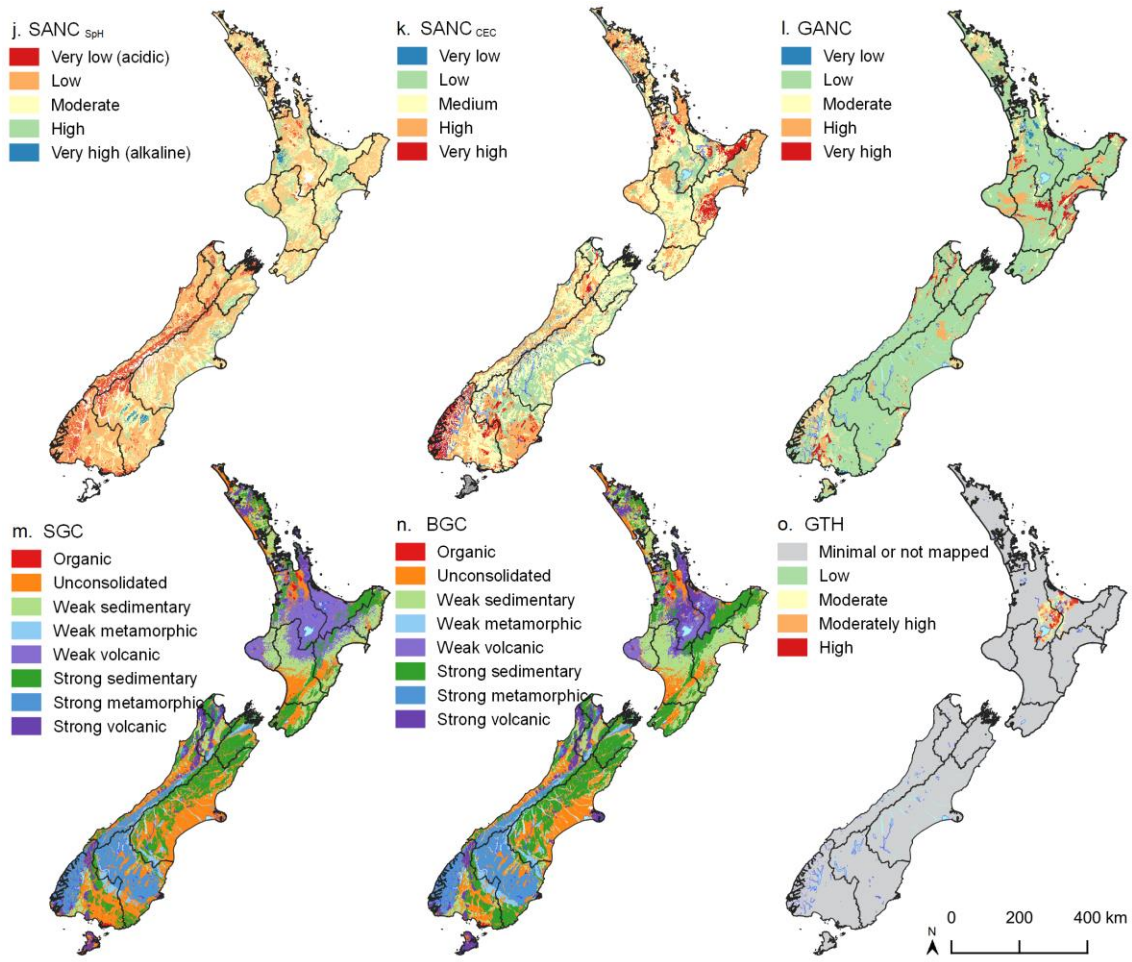

Figure 4 continued. Examples of process attribute gradients representing the 4 dominant processes. j) weathering (chemical) showing soil acid neutralizing capacity by pH, k) soil acid neutralizing capacity by cation exchange capacity, l) geological acid neutralizing capacity, m) weathering (physical) showing surface lithology and rock strength, n) basal lithology and rock strength, and o) geothermal process showing resistivity for the Taupo Volcanic Zone. Acronyms are defined in **Table 2**.

5.2 Hypothesis testing and representativeness evaluation

The performance of PoAM to replicate the effective atmospheric, hydrological, redox, and weathering gradients across the seven regions is presented in **Table 3**. Machine-defined functions for the dominant processes responded as hypothesised, and except for clarity (R^2 0.52), cross-validated R^2 values of 0.61 to 0.84 indicate moderate to very good representation of macro- and mesoscale hydrological gradients and mesoscale redox and chemical weathering gradients (**Table 3**).

ESSOAr | https://doi.org/10.1002/essoar.10507536.1 | CC_BY_4.0 | This content has not been peer reviewed.

Table 3. Cross-validated performance of process-attribute gradients to estimate hydrochemical tracers of each dominant process across 7-regions.

Process	Tracer	R^2	Correlation Coefficient	Maximum Error	Mean Squared Error	Mean Absolute Error	Complexity
Hydrology	Cl	0.69	0.83	1.98	0.24	0.36	57
	Br	0.70	0.83	1.89	0.21	0.32	78
	K	0.73	0.86	1.99	0.20	0.30	72
Redox	FeII	0.61	0.79	2.78	0.32	0.36	31
	DOC	0.80	0.90	2.53	0.25	0.33	26
Chemical Weathering	Total Alkalinity	0.71	0.84	2.07	0.28	0.39	35
	Ca	0.67	0.82	2.55	0.25	0.35	33
	$SiO_{2(aq)}$	0.84	0.92	1.87	0.19	0.32	59
Physical Weathering	Clarity	0.76	0.88	1.67	0.15	0.23	48

DOC: dissolved organic carbon

As expected, performance at the regional subset-scale was significantly better than at the national-scale for all tracers (**Table 3 and 4**). The process-attribute gradients defined and retained, and their relative sensitivities, are presented for each regional subset in **Supporting Information 4**. At a high-level, macroscale precipitation source (O18), precipitation volume and recharge domain were retained as the most sensitive predictors of the conservative hydrological tracers Cl and Br; soil reduction potential, soil drainage class equivalents and geological reduction potential were retained as the most sensitive predictors of the redox tracers FeII and DOC, and; soil and geological acid neutralisation capacity were retained as the most sensitive predictors of total alkalinity, Ca and dissolved reactive silica ($SiO_{2(aq)}$). As we hypothesised, the atmospheric and hydrological process-attribute gradients were retained alongside redox and chemical weathering tracers as sensitive predictors of observed spatial variation. The retention of atmospheric and hydrological process-attribute gradients reflects the important role of water source, precipitation volume and macroscale routing of water over spatial variation in redox and weathering process signals. Although machine-defined functions for each dominant process responded as hypothesised, significant variation in the process-attribute gradients retained and their relative sensitivities were observed between regional subsets (see **S4**).

Table 4. Model performance for hydrochemical tracers of dominant processes across regional subsets.

Tracer	Regional Subset	R^2	Correlation Coefficient	Maximum Error	Mean Squared Error	Mean Absolute Error	Complexity
Cl	Northland - Auckland	0.82	0.91	0.77	0.04	0.13	45
	Waikato - Bay of Plenty	0.71	0.85	1.74	0.14	0.24	41
	Manawatu	0.84	0.92	0.87	0.06	0.18	47
	Canterbury	0.79	0.89	1.87	0.18	0.26	53
	Southland	0.95	0.98	0.74	0.05	0.16	22
Br	Northland - Auckland	0.74	0.87	0.94	0.16	0.31	66
	Waikato - Bay of Plenty	.	.	.	.	.	.
	Manawatu	0.78	0.88	1.93	0.11	0.19	38
	Canterbury	0.71	0.85	1.92	0.25	0.34	74
	Southland	0.87	0.93	1.65	0.13	0.19	37
K	Northland - Auckland	0.79	0.89	0.82	0.06	0.17	30
	Waikato - Bay of Plenty	0.84	0.92	1.82	0.17	0.26	36
	Manawatu	0.77	0.88	1.61	0.12	0.19	42
	Canterbury	0.86	0.86	0.86	0.86	0.86	50
	Southland	0.80	0.90	1.17	0.05	0.14	34
FeII	Northland - Auckland	0.71	0.85	3.37	0.39	0.33	58
	Waikato - Bay of Plenty	0.95	0.97	0.48	0.03	0.13	57
	Manawatu	0.79	0.90	0.20	0.01	0.05	53
	Canterbury	0.56	0.80	2.35	0.17	0.19	44
	Southland	0.87	0.93	1.65	0.11	0.23	37
DOC	Northland - Auckland	0.74	0.87	1.72	0.10	0.17	57
	Waikato - Bay of Plenty	.	.	.	.	.	.
	Manawatu	0.82	0.91	1.12	0.07	0.16	40
	Canterbury	0.54	0.74	2.09	0.18	0.25	42
	Southland	0.96	0.98	0.98	0.06	0.16	38
Total Alkalinity	Northland - Auckland	0.66	0.82	1.41	0.23	0.34	45
	Waikato - Bay of Plenty	0.81	0.90	1.09	0.09	0.22	51
	Manawatu	0.75	0.87	2.55	0.33	0.36	48
	Canterbury	0.78	0.88	1.45	0.18	0.32	27
	Southland	0.92	0.96	0.80	0.06	0.17	47
Ca	Northland - Auckland	0.71	0.86	1.64	0.15	0.25	44
	Waikato - Bay of Plenty	0.75	0.87	1.58	0.13	0.24	34
	Manawatu	0.88	0.94	1.05	0.11	0.23	47
	Canterbury	0.75	0.87	2.76	0.30	0.36	72
	Southland	0.93	0.96	0.91	0.06	0.16	38
$SiO_{2(aq)}$	Northland - Auckland	0.62	0.79	1.07	0.11	0.22	38
	Waikato - Bay of Plenty	0.86	0.96	0.84	0.09	0.20	38
	Manawatu	0.80	0.90	0.86	0.08	0.18	43
	Canterbury	0.78	0.89	1.06	0.07	0.17	42
	Southland	0.78	0.89	0.84	0.05	0.16	37
Clarity	Northland - Auckland	0.93	0.96	0.11	0.00	0.03	31
	Waikato - Bay of Plenty	0.67	0.82	0.48	0.02	0.11	27
	Manawatu	0.72	0.86	0.41	0.02	0.10	78
	Canterbury	0.52	0.72	0.63	0.05	0.16	48
	Southland	0.82	0.91	0.59	0.01	0.08	31

ESSOAr | https://doi.org/10.1002/essoar.10507536.1 | CC_BY_4.0 | This content has not been peer reviewed.

5.3 Performance of process-attribute gradients to predict water quality

The observed sensitivities and associated magnitude of response of process-attribute gradients supported the high-level hypotheses, so land-use gradients (**Fig. 3b**) were incorporated, and water quality models were developed for each regional subset. Median cross-validated performance measures were calculated from regional subsets and are summarized in **Table 5**. Median performance measures include a cross-validated R^2 of 0.78 for total nitrogen, 0.79 for nitrate-nitrite nitrogen, 0.73 for total phosphorus, 0.73 for dissolved reactive phosphorus, 0.69 for turbidity (Nephelometric turbidity units), 0.62 for clarity (black disk), and 0.74 for *E. coli*. The regional subset performance measures are presented in **Table 6** and retained process-attribute gradients and sensitivities provided in **Supporting Information 5**.

Table 5. Median cross-validated performance measures for 811 water quality sites nationally.

	TN	NNN	TP	DRP	Turb.	Clarity	*E. coli*
R^2	0.78	0.79	0.73	0.73	0.69	0.62	0.74
Correlation coefficient	0.89	0.89	0.85	0.86	0.83	0.79	0.87
Maximum error	0.59	0.85	0.65	0.58	0.74	0.55	0.90
Mean squared error	0.03	0.10	0.03	0.04	0.05	0.02	0.07
Mean absolute error	0.13	0.21	0.11	0.12	0.15	0.11	0.19
Complexity	33	42	38	38	42	35	35

DRP: Dissolved Reactive Phosphorus; *E. Coli*: bacterial indicator; NNN: Nitrate-Nitrite Nitrogen; TN: Total Nitrogen; TP: Total Phosphorus; Turb.: Turbidity in Nephelometric Units.

In terms of sensitivity, the gradients retained for each water quality measure and each regional subset were, overall, consistent with expert knowledge. For example, artificial drainage and soil reduction potential process-attribute gradients were amongst the most sensitive predictors of nitrate-nitrite nitrogen (negative magnitude), total phosphorus, and dissolved reactive phosphorus (positive magnitude) across regional subsets; regolith cohesion status process-attribute gradients were amongst the most sensitive predictors of total phosphorus, dissolved reactive phosphorus (positive magnitudes), clarity (negative magnitude) and, to a lesser degree, turbidity (positive magnitude). Artificial drainage and natural bypass (cracking soils) were amongst the most sensitive predictors of *E. coli* (positive magnitudes). Normalized by the area of developed land, overland flow exhibited a positive magnitude for most water quality measures. Overall, land-use intensity process-attribute gradients were retained as the most sensitive predictors of total nitrogen and nitrate-nitrite nitrogen and *E. coli* (positive magnitudes) but were less commonly retained and of lower sensitivity for total phosphorus, dissolved reactive phosphorus, turbidity (NTU), and clarity. However, regional subsets showed significant variation in performance measures and process-attribute gradients retained by the statistical model.

Table 6. The cross-validated performance measures for 811 water quality sites by regional subset.

Analyte	Regional Subset	R^2	Correlation Coefficient	Maximum Error	Mean Squared Error	Mean Absolute Error	Complexity
TN	Northland - Auckland	0.90	0.95	0.38	0.01	0.06	33
	Waikato - Bay of Plenty	0.81	0.90	0.79	0.03	0.12	39
	Wellington-Manawatu-Taranaki	0.78	0.89	0.57	0.03	0.13	19
	Hawkes Bay - Gisborne	0.74	0.87	0.73	0.04	0.13	23
	West Coast-Tasman-Nelson	0.75	0.87	0.59	0.04	0.14	86
	Marlborough-Canterbury	0.71	0.85	0.71	0.10	0.24	17
	Southland - Otago	0.86	0.93	0.54	0.03	0.12	41
NNN	Northland - Auckland	0.83	0.92	0.78	0.06	0.15	23
	Waikato - Bay of Plenty	0.82	0.91	0.67	0.05	0.16	43
	Wellington-Manawatu-Taranaki	0.81	0.90	0.83	0.05	0.17	25
	Hawkes Bay - Gisborne	0.73	0.86	0.99	0.10	0.21	29
	West Coast-Tasman-Nelson	0.79	0.89	1.02	0.10	0.21	44
	Marlborough-Canterbury	0.71	0.84	1.75	0.21	0.31	42
	Southland - Otago	0.79	0.89	0.85	0.11	0.25	42
TP	Northland - Auckland	0.83	0.92	0.38	0.02	0.08	30
	Waikato - Bay of Plenty	0.72	0.85	0.74	0.04	0.14	45
	Wellington-Manawatu-Taranaki	0.69	0.84	0.53	0.02	0.11	34
	Hawkes Bay - Gisborne	0.79	0.89	0.68	0.03	0.11	37
	West Coast-Tasman-Nelson	0.73	0.85	0.41	0.03	0.12	43
	Marlborough-Canterbury	0.63	0.80	0.65	0.05	0.16	29
	Southland - Otago	0.85	0.92	0.65	0.03	0.11	40
DRP	Northland - Auckland	0.66	0.85	0.58	0.04	0.11	16
	Waikato - Bay of Plenty	0.68	0.82	0.73	0.06	0.19	38
	Wellington-Manawatu-Taranaki	0.57	0.77	0.01	0.00	0.00	49
	Hawkes Bay - Gisborne	0.75	0.87	0.85	0.04	0.14	35
	West Coast-Tasman-Nelson	0.73	0.86	0.50	0.03	0.12	41
	Marlborough-Canterbury	0.74	0.86	0.60	0.06	0.19	35
	Southland - Otago	0.76	0.88	0.51	0.03	0.12	45
Turbidity (NTU)	Northland - Auckland	0.92	0.96	0.20	0.01	0.05	33
	Waikato - Bay of Plenty	0.69	0.83	0.85	0.05	0.15	58
	Wellington-Manawatu-Taranaki	0.66	0.81	0.76	0.05	0.15	26
	Hawkes Bay - Gisborne	0.59	0.78	0.45	0.03	0.11	45
	West Coast-Tasman-Nelson	0.74	0.86	0.74	0.06	0.17	66
	Marlborough-Canterbury	0.48	0.70	0.90	0.09	0.23	42
	Southland - Otago	0.81	0.90	0.54	0.03	0.11	40
Clarity (Black Disk)	Northland - Auckland	0.89	0.94	0.18	0.00	0.04	33
	Waikato - Bay of Plenty	0.73	0.85	0.49	0.02	0.10	37
	Wellington-Manawatu-Taranaki	0.66	0.82	0.47	0.02	0.11	35
	Hawkes Bay - Gisborne	0.61	0.78	0.40	0.02	0.09	40
	West Coast-Tasman-Nelson	0.62	0.79	0.55	0.04	0.14	29
	Marlborough-Canterbury	0.50	0.72	0.64	0.05	0.16	43
	Southland - Otago	0.58	0.77	0.66	0.04	0.12	29
E. coli	Northland - Auckland	0.74	0.87	0.39	0.02	0.09	42
	Waikato - Bay of Plenty	0.75	0.87	0.90	0.07	0.19	29
	Wellington-Manawatu-Taranaki	0.73	0.85	0.77	0.06	0.18	25
	Hawkes Bay - Gisborne	0.74	0.86	0.82	0.06	0.17	31
	West Coast-Tasman-Nelson	0.59	0.78	1.70	0.14	0.24	52
	Marlborough-Canterbury	0.74	0.87	1.24	0.11	0.25	39
	Southland - Otago	0.74	0.87	0.90	0.07	0.19	35

DRP: Dissolved Reactive Phosphorus; *E.coli*: bacterial indicator; NNN: Nitrate-Nitrite Nitrogen; TN: Total Nitrogen; TP: Total Phosphorus; Turb.: Turbidity in Nephelometric Units.

ESSOAr | https://doi.org/10.1002/essoar.10507536.1 | CC_BY_4.0 | This content has not been peer reviewed.

6 Discussion

6.1 The importance of localized geological and climatic histories over water composition

Due to New Zealand's geological diversity, it is unsurprising that the sensitivities of process-attribute gradients varied between regional subsets. For example, the geothermal process-attribute gradient was identified as the most sensitive predictor of $SiO_{2(aq)}$ across the Taupo Volcanic Zone which includes large areas of the Waikato and Bay of Plenty Regions (see **S4**). The geothermal process-attribute was also retained as a sensitive predictor of total carbonate alkalinity. The importance of the geothermal process-attribute gradient over $SiO_{2(aq)}$ and total alkalinity is consistent with the high partial pressures of CO_2 and dissolved silica within the hydrothermal fluids of the Taupo Volcanic Zone (Giggenbach, 1995). These fluids ascend and mix with the shallow meteoric aquifers and discharge via the surface water network. Outside the areas of high enthalpy geothermal activity, the majority of New Zealand soil and geological acid neutralizing capacity and regolith cohesion process-attribute gradients were retained as the most sensitive predictors of total alkalinity and dissolved reactive silica.

For water quality, annualized loads of total nitrogen and total phosphorus from the surface water network to 12 Bay of Plenty region lakes had geothermal contributions up to 29.5 and 68%, respectively (Donovan and Donovan, 2003). This reflects high concentrations of ammonium and phosphorus in hydrothermal fluids (Hamill, 2018; Giggenbach, 1995). As this assessment did not evaluate direct inputs of geothermal fluids from the lakebed, these estimates are likely conservative (see Hamill, 2018). Therefore, it is perhaps unsurprising that the geothermal process-attribute layer was retained as the most sensitive predictor of total nitrogen and dissolved reactive phosphorus (positive magnitudes) across both geothermally active regions within the Taupo Volcanic Zone (see **S5**). However, land use intensity was retained as the most sensitive predictor of nitrate-nitrite-nitrogen, probably because of the low redox potential of geothermal fluids, favoring ammoniacal nitrogen.

In another example, Northland and Auckland were the only regions for which the regolith cohesion status was retained as the most sensitive predictor of surface water turbidity (NTU) and clarity (see **S5**). Here, the regolith cohesion process-attribute gradient is ranked from low to high, with a negative magnitude of response recorded for turbidity and a positive magnitude of response for clarity, i.e., turbidity decreases, and clarity increases, as the cohesion status of the regolith increases. These regions are characterised as the oldest and most weathered in New Zealand, with no evidence of glaciation, widespread ash fall deposits or significant Quaternary tectonic activity (Richardson et al., 2013, 2014; Hayward, 2017). The antiquity of the landscape, an abundance of relatively unconsolidated sedimentary rocks relative to elsewhere in New Zealand, and Northland's subtropical climate have resulted in high rates of mass wasting and erosion in response to anthropogenic activity (Richardson et al., 2013, 2014; Swales et al., 2015; McDonald et al., 2020). Outside of Northland and Auckland, across the much larger area of geomorphically young landforms, macroscale precipitation source and volume, recharge domain and hydrological routing, mesoscale hydrological pathway (also of developed land), and both soil and geological acid neutralization capacity process-attribute gradients are more common predictors of turbidity and clarity (see **S5**). The retention of acid neutralization process-attribute gradients as sensitive predictors of turbidity and clarity is thought to reflect the association between weak calcareous mudstones and evidence in satellite imagery for higher mass-wasting rates (Rissmann et al., 2020a).

ESSOAr | https://doi.org/10.1002/essoar.10507536.1 | CC_BY_4.0 | This content has not been peer reviewed.

In one final example, Northland-Auckland and Southland-Otago regions contain the greatest proportion of imperfectly to poorly drained soils (for land < 12° slope) and the highest concentration of artificially drained (mole-pipe and ditch drainage) agricultural land nationally. Where artificial drainage is associated with reducing soil profile forms (e.g., gleysols or organic carbon dominated), redox conditions may enhance phosphorus mobility and associated export to surface waters (Scalenghe et al., 2010). An abundance of fine-textured and poorly permeable soils and shallow water tables also favors overland flow. Parsimoniously then, the artificial drainage density process-attribute gradient was retained as the most sensitive predictor of total and dissolved reactive phosphorus (positive magnitudes) across these two regional subsets (see **S5**). Those regional subsets with a smaller proportion of artificially drained soils retained water table, soil, and geological reduction potential as sensitive predictors of phosphorus loss.

In summary, differences in the geological and climatic evolution of a region can result in critical, regional-scale variability in water quality drivers. This variability may be lost when aggregating data for national models. For example, aggregating the hydrochemistry dataset from all regions into one model run, the key regional drivers of variation in the process signatures noted above were lost, and predictive uncertainty increased (**Table 3** versus **Table 4**).

6.2 PoAM performance

Multivariate evaluation shows that process-attribute gradients effectively replicated the dominant process gradients responsible for the generation, storage, attenuation, and transport of water quality contaminants in the environment. The observation that spatial variation in water composition can be reliably estimated as a function of landscape attributes is consistent with New Zealand and international studies (Johnson et al., 1997; Hale et al., 2004; Snelder and Biggs, 2002; Snelder et al., 2005; King et al., 2005; Dow et al., 2006; Becker et al., 2014; Rissmann et al., 2019).

Nonetheless, the identification of regional variations in process-attributes, and their relative sensitivities, are significant and represent regional-scale variability in geological and climatic histories. We consider it logical that regions with unique geological attributes or climatic histories (e.g., high-temperature geothermal activity, deeply weathered regolith, or a greater abundance of imperfectly to poorly drained soils) will respond differently to land-use pressures and/or have distinct endogenous sources of water quality contaminants. Our interpretation is consistent with observed regional variation in the type and severity of water quality issues across New Zealand (Ministry for the Environment & Stats NZ, 2020).

Overall, the validity and observed performance of the PoAM approach is supported by the dominant process concept proposed by Grayson and Blöschl (2001), namely:

i. that the response of environmental systems is commonly well explained by the representation of a small number of dominant processes.

ii. that a logical way to identify the dominant processes governing a system is by evaluating the sensitivity of the system to each of the individual processes (believed to have influence) through a (high-order) multi-variable sensitivity analysis and selecting those variables that are found to have a 'noticeably' significant influence (Sivakumar, 2004; 2008).

ESSOAr | https://doi.org/10.1002/essoar.10507536.1 | CC_BY_4.0 | This content has not been peer reviewed.

6.3 Limitations to Process-Attribute Mapping (PoAM)

Based on expert knowledge and machine defined relationships, process-attribute gradients provide a reasonable approximation of the macroscale process gradients that govern the generation, storage, attenuation, and transport of water quality contaminants. However, as with any complex system, the ability to isolate and depict first-order drivers of process response is challenging. Accordingly, as with any model each process-attribute layer can only be considered an approximation of the 'real' macroscale process-attribute gradient.

In addition to the challenges of isolating first-order drivers of process response, spatial correlation between landscape attributes may interfere with the machine-driven isolation of primary drivers (Rissmann et al., 2019). This is especially true of process-attribute gradients that share similar landscape attributes. For example, both artificial drainage and soil redox potential include soil drainage class as one of the controlling landscape attributes. As a result, these two process-attribute gradients are spatially correlated ($R = 0.36$) despite representing different dominant processes, i.e., hydrological versus redox. In some settings, this may result in the artificial drainage layer being retained as an important predictor of redox sensitive species such as FeII and DOC. Although dissolved iron and DOC are commonly elevated in mole-pipe drainage from poorly drained soils (Rissmann and Beyer, 2016), it is incorrect to say that artificial drainage is a driver of low soil redox potential. In these situations, expert knowledge is an important basis for interpreting machine defined relationships.

Collinearity is also partially addressed during the evaluation of the sensitivity and magnitude of response of process-attribute gradients over a given hydrochemical tracer (**Fig. 1**, **Step 4**). Specifically, the HDGP method models each, possibly coupled, variable separately, intelligently perturbing and destabilising the system to extract its less observable characteristics and automatically simplifying the equations during modelling (Schmidt and Lipson, 2009, 2015). This feature of HDGP supports the identification of the most sensitive predictors or closest approximations of the actual process-attribute gradients governing a given hydrochemical tracer or water quality measure.

Besides revealing the hidden patterns underlying complex non-linear systems, our preference for HDGP relates to the important challenge of feature selection in high-dimensional data sets. For example, we note that Random Forests might overlook important variables. Specifically, the work of Stijven et al. (2011) noted that although Random Forests can efficiently find important variables, it may struggle to do so where many variables are equally important. Poor discrimination of variables with similar weightings results in the sensitivity of predictors varying randomly, given that such variables are not recognised as being truly distinct. Stijven et al. (2011) also noted that variable importance is influenced by data distribution, which can result in misinterpretation and concluded that caution is advised when using Random Forests to decide which variables to retain, even if the dataset is known not to exhibit strong correlations or unevenly balanced data. This is because data points in leaf nodes are similar in the nearest neighbour sense, and the variables selected by Random Forests express proximity. In comparison, HDGP more robustly identifies important variables if models of sufficient quality are found (Stijven et al., 2011; Icke and Bongard, 2013; Arnaldo et al., 2014; Schmidt and Lipson, 2009, 2015).

Another important feature of the machine defined sensitivity analysis employed here includes the development of a mathematically transparent model (i.e., "white box") of the

relationship between process-attribute gradients that minimises both model error and complexity (**Fig. 1 Step 4**). HDGP does this via randomly combining different mathematical building blocks (i.e., basic arithmetic operators, trigonometric and exponential functions) and assessing which combination provides the most accurate and least complex model. If a combination does not improve the accuracy of an estimate or reduce a model's complexity, it is discarded (Khu et al., 2001; Schmidt and Lipson, 2009, 2015). The same evolutionary approach operates on the predictors, whereby any process-attribute gradients that do not improve the accuracy and reduce the complexity of a model are discarded. Therefore, instead of offering a single model and calibrating it to the data, millions of possible models are evaluated and then calibrated as part of the evolutionary process. Here the ultimate objective is to converge upon a single solution that 'best' defines the relationship between process-attribute gradients and a target variable (i.e., a hydrochemical tracer). A desire for greater transparency over the relationships between drivers and system response has resulted in an increasing number of researchers applying symbolic methods to resolve better the drivers of complex, non-linear natural systems (Whigham and Crapper, 2001; Jagupilla et al., 2015; Chadalawada et al., 2017; Aryafar et al., 2019; Rajaee et al., 2020).

Testing bias is associated with the location of surface water monitoring sites for process-attribute gradient performance. These monitoring sites are associated with higher order streams (≥ 3) and larger drainage basin areas for pragmatic reasons. Specifically, of the 730 surface water capture zones with hydrochemical data, the median size is 122 km^2, with only 38 less than 5 km^2 (500 ha). This is relevant because 44 % of farms across New Zealand are less than 40 ha, with a further 48 % ranging between 40 and 600 ha (StatsNZ, 2018). The average farm size globally is even smaller at < 20 ha (Samberg et al., 2016). This is important given that error within most models tends to increase as drainage basin size decreases, reflecting increasing sensitivity to the resolution, and hence accuracy, at which landscape attributes and land use intensity gradients are depicted (Troy et al., 2008; Mattot et al., 2009; Moriasi et al., 2015). The loss of accuracy at small scales is particularly relevant given most geospatial layers used in this study were only as fine as 1:50,000 scale, with finer scales necessary for assessing controls at property scales. Currently, this work is primarily relevant to larger scales associated with higher-order streams (≥ 3).

6.4 Future work for process attribute mapping in New Zealand and globally

Improvements in the spatial resolution of process-attribute gradients by developing finer-scaled landscape attribute datasets. For example, airborne radiometric survey data (typically 50 x 50 m resolution) can be used to provide enhanced resolution over subsurface carbon stores and soil drainage properties (Beamish, 2014; Beamish, 2015). These, and other high-resolution data sets, can be used to provide better proxies of actual landscape gradients than are currently available (Rissmann et al., 2018c, 2020a, b; Rissmann and Pearson, 2020). A higher-resolution depiction of process-attribute gradients is critical for guiding investments to improve water quality outcomes at the small scale typical of most farms globally.

The process-attribute gradients developed would further benefit from the measurement of hydrochemical tracers in surface and ground water. For example, in New Zealand this could be done across the eight regions not included in this study. Such data would support the refinement of process-attribute gradients and potentially drive improved performance. High-quality classifications and datasets defining groundwater redox potential could be used to enhance the

ESSOAr | https://doi.org/10.1002/essoar.10507536.1 | CC_BY_4.0 | This content has not been peer reviewed.

representativeness of the geological reduction potential layer (Collins et al., 2017; Rivas et al., 2017; Burbery, 2018; Martindale et al., 2019; Wilson et al., 2020). Approximations of unsaturated zone and saturated zone lags could also be generated to better account for the important control of 'time' over spatial variation in water quality (see Wilson et al., 2014).

Future work will focus on developing an integrated classification that groups areas with the similar process-attribute classes into a single class. Each class is theorised to respond in a similar fashion at the process level to broadly equivalent land use pressure, generating predictable water quality outcomes (see Hughes et al., 2016; Rissmann et al., 2018a).

Globally, similar datasets exist or could be developed to apply PoAM. Examples include national or regional climatic, geologic, soil and hydrological datasets. Hydrochemical data can be collected, if not already available, and used to guide classification. For areas lacking hydrochemical data, controlling landscape attribute hypothesises can be developed using relevant literature and local knowledge from which a top-down process-attribute classification could be built. Such a classification could then be used to guide an efficient sampling campaign. Data collected from such a survey could be used to refine existing hypothesis and improve the representation of dominant process gradients.

7 Conclusions

Process-attribute mapping (PoAM) utilises signals within water to map four dominant processes that, in combination with land use, govern the generation, storage, attenuation and transport of contaminants in the environment. The performance of PoAM to estimate wide-ranging hydrochemical and water quality measures across the diverse landscape of New Zealand highlights the utility of the method. Recognizing that regions with unique geological attributes and climatic histories respond differently to land-use pressures and/or have distinct endogenous sources of contaminants is critical to model, and subsequently improve, water quality. Models or policies that fail to consider landscape variation will misidentify governing factors and produce outputs or rule frameworks that may not support improved water quality.

Uncertainties associated with PoAM as tested in New Zealand reflect the spatial coarseness of the surface water monitoring network used to assess performance and the resolution of the input datasets that typically were created for purposes other than water quality. For this reason, the outputs in this study are primarily relevant to larger scales associated with higher-order streams (≥3) but could be significantly improved by higher-resolution input datasets. The PoAM approach is here demonstrated to be useful in modelling water quality in the complex New Zealand landscape, and could be equally applicable in other countries with or without similar landscape diversity. Future research seeks to refine and further validate the PoAM approach, and to develop an integrated classification that groups areas with the same process-attribute gradients into distinct physiographic environments. Globally, many countries possess equivalent datasets that could be used to support the application of PoAM.

ESSOAr | https://doi.org/10.1002/essoar.10507536.1 | CC_BY_4.0 | This content has not been peer reviewed.

Acknowledgments

The median hydrochemical (surface and groundwater) and water quality (surface water) data used to guide the classification of process attribute gradients and the associated mean PAG scores used in model development and evaluation in this study are available at Mendeley Data, New Zealand Process Attribute Mapping via doi: 10.17632/mhmbmmk5cv.1 and doi: 10.17632/62vws535pt.1, respectively. Both datasets are available under CC by 4.0. Process-attribute gradient maps are available to view at www.landscapedna.org.

We acknowledge funding contribution and investment in hydrochemical data collection in Northland, Auckland, Waikato, Bay of Plenty, Manawatu-Whanganui, Canterbury, and Southland Regions by the regional authorities. The development of a national scale Physiographic Environment classification for water quality is part of a 3-year project funded by New Zealand's Our Land and Water National Science Challenge to support improved water quality outcomes. We thank Matthew Couldrey and Jessie Lindsay for GIS support and Ton Snelder and Brydon Hughes for valuable discussion that helped refine the content of this manuscript.

ESSOAr | https://doi.org/10.1002/essoar.10507536.1 | CC_BY_4.0 | This content has not been peer reviewed.

References

Aho, K., Derryberry, D., & Peterson, T. (2014). Model selection for ecologists: the worldviews of AIC and BIC. *Ecology*, 95(3): 631-636.

Arnaldo, I., Krawiec, K. & O'Reilly, U.M. (2014). Multiple regression genetic programming. In *Proceedings of the 2014 Annual Conference on Genetic and Evolutionary Computation* (pp. 879-886).

Aryafar, A., Khosravi, V., Zarepourfard, H., & Rooki, R. (2019). Evolving genetic programming and other AI-based models for estimating groundwater quality parameters of the Khezri plain, Eastern Iran. *Environmental Earth Sciences*, 78(3), 69.

Baisden, W.T., Keller, E.D., Van Hale, R., Frew, R.D., & Wassenaar, L.I. (2016). Precipitation isoscapes for New Zealand: enhanced temporal detail using precipitation-weighted daily climatology. *Isotopes in Environmental and Health Studies*, 52(4-5): 343-352.

Beamish, D. (2014). Peat mapping associations of airborne radiometric survey data. *Remote Sensing*, 6(1): 521-539.

Beamish, D. (2015). Relationships between gamma-ray attenuation and soils in SW England. *Geoderma*, 259-260: 174-186.

Becker, J. C., Rodibaugh, K. J., Labay, B. J., Bonner, T. H., Zhang, Y., & Nowlin, W. H. (2014). Physiographic gradients determine nutrient concentrations more than land use in a Gulf Slope (USA) river system. *Freshwater Science*, 33(3), 731–744. https://doi.org/10.1086/676635

Beyer, M., Rissmann, C., Rodway, E., Killick, M., & Pearson, L. (2016a). Technical Chapter 6: Influence of Soil and Geological Composition over Redox Conditions for Southland Groundwater and Surface Waters. Environment Southland, Invercargill, New Zealand (2016) Technical Report. No: 2016/3.

Beyer, M., Rissmann, C., Rodway, E., Marapara, T.R., Hodgetts, J. (2016b). Technical Chapter 2: Discrimination of Recharge Mechanism and Vulnerability to Bypass Flow. Environment Southland, Invercargill, New Zealand (2016) Technical Report. No: 2016/3.

Bibby, H.M., Caldwell, T.G., Davey, F.J. & Webb, T.H. (1995). Geophysical evidence on the structure of the Taupo Volcanic Zone and its hydrothermal circulation. *Journal of Volcanology and Geothermal Research*, 68(1-3), pp.29-58.

Burbery, L. (2018). Nitrate reactivity in groundwater: a brief review of the science, practical methods of assessment, and collation of results from New Zealand field investigations. *Journal of Hydrology (New Zealand)*, 57(2), p.41.

Chadalawada, J., Havlicek, V. & Babovic, V. (2017). A genetic programming approach to system identification of rainfall-runoff models. *Water Resources Management*, 31(12), pp.3975-3992.

Clark, I.D., & Fritz, P. (1997). Environmental Isotopes in Hydrogeology. CRC press.

Close, M. E., Abraham, P., Humphries, B., Lilburne, L., Cuthill, T., & Wilson, S. (2016). Predicting groundwater redox status on a regional scale using linear discriminant analysis. *Journal of Contaminant Hydrology*, Vol. 16(12), 4760-66

Collins, S., Singh, R., Rivas, A., Palmer, A., Horne, D., Manderson, A., Roygard, J., & Matthews, A. (2017). Transport and potential attenuation of nitrogen in shallow groundwater in the lower Rangitikei catchment, New Zealand. *Journal of Contaminant Hydrology*, 206: 55-66. DOI 10.1016/j.jconhyd.2017.10.002

Daughney, C., Rissmann, C., Friedel, M., Morgenstern, U., Hodson, R., van der Raaij, R., Rodway, E., Martindale, H., Pearson, L., Townsend, D., Kees, L., Moreau, M., Millar, R., Horton, T. (2015). Hydrochemistry of the Southland Region, GNS Science Report 2015/24.

Davies-Colley, R.J., Hughes, A.O., Verburg, P, & Storey, R. (2012). Freshwater Monitoring Protocols and Quality Assurance (QA) National Environmental Monitoring and Reporting (NEMaR) Variables Step 2. Prepared for the Ministry for the Environment. NIWA Client report HAM2012-092. 104p

de Sousa, L.M., Poggio, L., Dawes, G., Kempen, B., & van den Bosch, R. (2020). Computational Infrastructure of SoilGrids 2.0. In: Athanasiadis, I.N., Frysinger, S.P., Schimak, G., Knibbe, W.J. (Editors), Environmental Software Systems. Data Science in Action. Springer International Publishing, Cham, pp. 24-31.

Dinerstein, E., Olson, D., Joshi, A., Vynne, C., Burgess, N.D., Wikramanayake, E., Hahn, N., Palminteri, S., Hedao, P., Noss, R. & Hansen, M. (2017). An ecoregion-based approach to protecting half the terrestrial realm. *BioScience*, 67(6), pp.534-545.

Donovan, C.L. & Donovan, W.F. (2003). Estimate of the Geothermal Nutrient Inputs to Twelve Rotorua Lakes. Bioresearches, Consulting Biologists & Archaeologists.

Dow, C.L., Arscott, D.B. & Newbold, J.D. (2006). Relating major ions and nutrients to watershed conditions across a mixed-use, water-supply watershed. *Journal of the North American Benthological Society*, 25(4), pp.887-911.

Drever, J.I. & Stillings, L.L. (1997). The role of organic acids in mineral weathering. *Colloids and Surfaces A: Physicochemical and Engineering Aspects*, 120(1-3), pp.167-181.

Dubčáková, R. (2011). Eureqa: software review. *Genetic Programming and Evolvable Machines*, 12(2): 173-178.

Edbrooke, S.W., Heron, D.W., Forsyth, P.J., & Jongens, R. (2015). Geological map of New Zealand 1:1 000 000. GNS Science Geological Map 2. 2 sheets. GNS Science, Lower Hutt, New Zealand.

European Commission. (2000). Directive 2000/60/EC. Establishing a framework for community action in the field of water policy. European Commission PE-CONS 3639/1/100 Rev 1, Luxembourg.

Geographx Ltd. (2009). NZ Landcover (100m). https://koordinates.com/layer/513-nz-landcover-100m/

Giggenbach, W.F. (1995). Variations in the chemical and isotopic composition of fluids discharged from the Taupo Volcanic Zone, New Zealand. *Journal of Volcanology and Geothermal Research*, 68(1-3), pp.89-116.

Grayson, R. & Blöschl, G. (2001). Spatial patterns in catchment hydrology: observations and modelling. CUP Archive.

Güler, C., Thyne, G.D., McCray, J.E., & Turner, K.A. (2002). Evaluation of graphical and multivariate statistical methods for classification of water chemistry data. *Hydrogeology Journal*, 10(4): 455-474.

Hale, S.S., Paul, J.F. & Heltshe, J.F. (2004). Watershed landscape indicators of estuarine benthic condition. *Estuaries*, 27(2), pp.283-295.

Hamill,K. D. (2018). Anthropogenic phosphorus load to Rotorua review and revision. Report for Bay of Plenty Regional Council. River Lake Ltd. 31p

Matott, L.S., Babendreier, J.E., & Purucker, S.T. (2009). Evaluating uncertainty in integrated environmental models: a review of concepts and tools. *Water Resources Research*, 45(6).

Hayward, B.W. (2017). Out of the Ocean, Into the Fire: History in the rocks, fossils and landforms of Auckland, Northland and Coromandel. Geoscience Society of New Zealand.

Hem, J.D. (1985). Study and interpretation of the chemical characteristics of natural water (Vol. 2254). Department of the Interior, US Geological Survey.

Heron, D.W. (2014). Geological map of New Zealand 1:250,000. GNS Science. GNS Science geological map 1, Lower Hutt, New Zealand

Hughes, R. M. & Larsen, D. P. (1988). Ecoregions: An approach to surface water protection. *Journal Water Pollution Control Federation*, 60: 486–493.

Hughes, B., Wilson, K., Rissmann, C. & Rodway, E. (2016). Physiographics of Southland: Development and application of a classification system for managing land use effects on water quality in Southland. Environment Southland, Invercargill, New Zealand (2016) Technical Report. No: (2016/11).

Icke, I. & Bongard, J.C. (2013). Improving genetic programming based symbolic regression using deterministic machine learning. In 2013 IEEE Congress on Evolutionary Computation (pp. 1763-1770). IEEE.

Inamdar, S. (2011). The use of geochemical mixing models to derive runoff sources and hydrologic flow paths. In Forest Hydrology and Biogeochemistry (pp. 163-183). Springer, Dordrecht.

Jagupilla, S.C.K., Vaccari, D.A., Miskewitz, R., Su, T.L. & Hires, R.I. (2015). Symbolic regression of upstream, stormwater, and tributary E. coli concentrations using river flows. *Water Environment Research*, 87(1), pp.26-34.

James, A. L. & Roulet, N. T. (2006). Investigating the applicability of end-member mixing analysis (EMMA) across scale: A study of eight small, nested catchments in a temperate forested watershed, *Water Resources Research*, 42, W08434, doi:10.1029/2005WR004419.

Johnson, L., Richards, C., Host, G. & Arthur, J. (1997). Landscape influences on water chemistry in Midwestern stream ecosystems. *Freshwater Biology*, 37(1), pp.193-208.

Kendall, C. & McDonnell, J.J. eds. (2012). Isotope Tracers in Catchment Hydrology. Elsevier.

Khu, S.T., Liong, S.Y., Babovic, V., Madsen, H., Muttil, N. (2001). Genetic programming and its application in real-time runoff forecasting 1. *JAWRA Journal of the American Water Resources Association*, 37(2): 439-451.

King, R.S., Baker, M.E., Whigham, D.F., Weller, D.E., Jordan, T.E., Kazyak, P.F. & Hurd, M.K. (2005). Spatial considerations for linking watershed land cover to ecological indicators in streams. *Ecological Applications*, 15(1), pp.137-153.

Krantz, D.E., & Powars, D.S. (2000). Hydrogeologic setting and potential for denitrification in ground water, coastal plain of southern Maryland. US Department of the Interior, US Geological Survey.

Kurtzman, D., Baram, S., & Dahan, O. (2016). Soil–aquifer phenomena affecting groundwater under vertisols: a review. *Hydrology and Earth System Sciences*, 20(1): 1.

Land Information New Zealand. (2012). NZ 8m Digital Elevation Model (2012). https://data.linz.govt.nz/layer/51768-nz-8m-digital-elevation-model-2012/

Leybourne, M.I. and Goodfellow, W.D. (2010). Geochemistry of surface waters associated with an undisturbed Zn–Pb massive sulfide deposit: water–rock reactions, solute sources and the role of trace carbonate. *Chemical Geology*, 279(1-2), pp.40-54.

Lynn, I.H., Manderson, A.K., Page, M.J., Harmsworth, G.R., Eyles, G.O., Douglas, G.B., Mackay, A.D., & Newsome, P.J.F. (2009). Land Use Capability Survey Handbook – A New Zealand Handbook for the Classification of Land. AgResearch Hamilton; Manaaki Whenua Lincoln; GNS Science, Lower Hutt, New Zealand.

Manaaki Whenua Landcare Research (2019a). S-map - New Zealand's national digital soil map. https://doi.org/10.7931/L1WC7.

Manaaki Whenua Landcare Research. (2019b). LCDB v5.0 - Land Cover Database version 5.0, Mainland New Zealand. https://lris.scinfo.org.nz/layer/104400-lcdb-v50-land-cover-database-version-50-mainland-new-zealand/

Manaaki Whenua Landcare Research. (2000a). NZLRI North Island, Edition 2 (all attributes). https://lris.scinfo.org.nz/layer/48134-nzlri-north-island-edition-2-all-attributes/

Manaaki Whenua Landcare Research. (2000b). NZLRI South Island, Edition 2 (all attributes). https://lris.scinfo.org.nz/layer/48135-nzlri-south-island-edition-2-all-attributes/

Manaaki Whenua Landcare Research. (2000c). FSL New Zealand Soil Classification. https://lris.scinfo.org.nz/layer/48079-fsl-new-zealand-soil-classification/

Martindale, H., van der Raaij, R., Daughney, C.J., Singh, R., Jha, N. & Hadfield, J. (2019). Assessment of excess N2 for quantifying actual denitrification in New Zealand groundwater systems. *Journal of Hydrology (New Zealand)*, 58(1), p.1.

McDonald, L., Pearson, L. & Rissmann, C. (2020). Validation of the Northland Sediment Process-Attribute Layer: Erosion Susceptibility Classification. Land and Water Science Report 2020/02. p26.

McMahon, P., & Chapelle, F. (2008). Redox processes and water quality of selected principal aquifer systems. *Groundwater*, 46(2): 259-271.

Ministry for the Environment. (2016). Average annual rainfall, 1972–2013. https://data.mfe.govt.nz/layer/53314-average-annual-rainfall-19722013/

Ministry for the Environment. (2019). LUCAS NZ Land Use Map 1990 2008 2012 2016 v006. https://data.mfe.govt.nz/layer/52375-lucas-nz-land-use-map-1990-2008-2012-2016-v006/

ESSOAr | https://doi.org/10.1002/essoar.10507536.1 | CC_BY_4.0 | This content has not been peer reviewed.

Ministry for the Environment & Stats NZ. (2020). New Zealand's Environmental Reporting Series: Our Freshwater 2020. Available from www.mfe.govt.nz and www.stats.govt.nz.

Moldan, B., & Černý, J. V. (1994). Biogeochemistry of small catchments: a tool for environmental research. Chichester, England, UK: John Wiley and Sons Ltd.

Moriasi, D.N., Gitau, M.W., Pai, N. & Daggupati, P. (2015). Hydrologic and water quality models: Performance measures and evaluation criteria. *Transactions of the ASABE*, 58(6), pp.1763-1785.

Mueller, E.R. & Pitlick, J. (2013). Sediment supply and channel morphology in mountain river systems: 1. Relative importance of lithology, topography, and climate. Journal of Geophysical Research: *Earth Surface*, 118(4), pp.2325-2342.

Newsome, P.F.J., Wilde, R.H., & Willoughby, E.J. (2008). Land Resource Information System Spatial Data Layers. Landcare Research, Palmerston North, New Zealand.

Nichol, S.E., Harvey, M.J. & Boyd, I.S. (1997). Ten years of rainfall chemistry in New Zealand. *Clean Air: Journal of the Clean Air Society of Australia and New Zealand*, 31(1), p.30.

Omernik, J.M., & Griffith, G.E. (2014). Ecoregions of the Conterminous United States: Evolution of a Hierarchical Spatial Framework. Environmental Management, 54(6): 1249-1266.

Panno, S.V., Hackley, K.C., Hwang, H.H., Greenberg, S., Krapac, I.G., Landsberger, S. & O'Kelly, D.J. (2002). Source identification of sodium and chloride contamination in natural waters: preliminary results. In Proceedings, 12th Annual Illinois Groundwater Consortium Symposium. Illinois Groundwater Consortium.

Pearson, L. (2015a). Overland flow risk in Southland. Environment Southland, Invercargill, New Zealand (2015) Technical Report. No:2015-06-2. 19p.

Pearson, L. (2015b). Artificial subsurface drainage in Southland. Environment Southland, Invercargill, New Zealand (2015) Technical Report. No: 2015-07. 20p.

Pearson, L. & Rissmann, C. (2021a). New Zealand Process Attribute Mapping: Hydrochemical surface and groundwater data (2007-2017), Mendeley Data, V1, doi: 10.17632/mhmbmmk5cv.1

Pearson, L. & Rissmann, C. (2021b). New Zealand Process Attribute Mapping: National surface water quality (2014-2018), Mendeley Data, V1, doi: 10.17632/62vws535pt.1

Rajaee, T., Khani, S., & Ravansalar, M. (2020). Artificial intelligence-based single and hybrid models for prediction of water quality in rivers: A review. *Chemometrics and Intelligent Laboratory Systems*, 200, 103978.

Richardson, J.M., Fuller, I.C., Holt, K.A., Litchfield, N.J. & Macklin, M.G. (2014). Rapid post-settlement floodplain accumulation in Northland, New Zealand. *Catena*, 113, pp.292-305.

Richardson, J.M., Fuller, I.C., Holt, K.A., Litchfield, N.J. & Macklin, M.G. (2013). Holocene river dynamics in Northland, New Zealand: The influence of valley floor confinement on floodplain development. *Geomorphology*, 201, pp.494-511.

ESSOAr | https://doi.org/10.1002/essoar.10507536.1 | CC_BY_4.0 | This content has not been peer reviewed.

Rissmann, C. (2011). Regional mapping of groundwater denitrification potential and aquifer sensitivity. Environment Southland, Invercargill, New Zealand (2011) Technical Report. No: 2011-12.

Rissmann, C. (2012). The Extent of Nitrate in Southland Groundwaters. Environment Southland, Invercargill, New Zealand (2012) Technical Report.

Rissmann, C., & Beyer, M. (2016). Tile drain and soil water sample assessment: relationships between soil denitrification potential and redox processes. GNS Science Report: SR 2016-060.

Rissmann, C., & Pearson, L. (2020). Physiographic Controls over Water Quality State for the Northland Region. Land and Water Science Report 2020/05. p120.

Rissmann, C., Rodway, E., Beyer, M., Hodgetts, J., Pearson, L., Killick, M., Marapara, T.R., Akbaripasand, A., Hodson, R., Dare, J., Millar, R., Ellis, T., Lawton, M., Ward, N., Hughes, B., Wilson, K., McMecking, J., Horton, T., May, D., & Kees, L. (2016a). Physiographics of Southland Part 1: Delineation of key drivers of regional hydrochemistry and water quality. Environment Southland, Invercargill, New Zealand. Technical Report No. 2016/3.

Rissmann, C., Rodway, E., Beyer, M., Marapara, T.R., Hodgetts, J., Pearson, L., & Killick, M. (2016b). Technical Chapter 5: Comparison of Soil Water with Surface Water and Groundwater Chemistry. Environment Southland, Invercargill, New Zealand (2016) Technical Report. No: 2016/3.

Rissmann, C., Pearson, L., Lindsay, J., Marapara, T., Badenhop, A., Couldrey, M., & Martin, A., (2018a). Integrated landscape mapping of water quality controls for farm planning - applying a high resolution physiographic approach to the Waituna Catchment, Southland. In: Farm environmental planning - Science, policy and practice. (Eds. L. D. Currie & C.L. Christensen). http:flrc.massey.ac.nz/publications.html. Occasional Report No. 31. Fertilizer and Lime Research Centre, Massey University, Palmerston North, New Zealand. 19 pages.

Rissmann, C., Pearson, L., Lindsay, J., Couldrey, M., & Lovett, A. (2018b). Application of Physiographic Science to the Northland Region: Preliminary Hydrological and Redox Process-Attribute Layers. Land and Water Science Report 2018/11. p88.

Rissmann, C., Pearson, L., Lindsay, J., & Couldrey, M. (2018c). Sediment Process-Attribute Layer for Northland. Land and Water Science Report 2018/35. p71

Rissmann, C.W.F., Pearson, L.K., Beyer, M., Couldrey, M.A., Lindsay, J.L., Martin, A.P., Baisden, W.T., Clough, T.J., Horton, T.W. & Webster-Brown, J.G. (2019). A hydrochemically guided landscape classification system for modelling spatial variation in multiple water quality indices: Process-attribute mapping. *Science of the Total Environment*, 672, pp.815-833.

Rissmann, C., Pearson, L., Shi, Y., & Lawrence, C. (2020a). Radiometric and Terrain Derived Erosion Susceptibility Classification for the Southland Region. Land and Water Science Report 2020/28. p82.

Rissmann, C., Pearson, L., Joy, K., & Dean, R. (2020b). Mapping Wetness Gradients utilising Radiometric and Satellite Imagery. Land and Water Science Report 2020/10. p58.

Rivas, A., Singh, R., Horne, D., Roygard, J., Matthews, A., & Hedley, M. (2017). Denitrification potential in the subsurface environment in the Manawatu River catchment, New Zealand: Indications from oxidation-reduction conditions, hydrogeological factors, and implications for nutrient management. *Journal of Environment Management*, 197, 476-489.

Rodway, E., Rissmann, C., Beyer, M., Marapara, T.R., & Hodgetts, J. (2016). Technical Chapter 1: Precipitation. Environment Southland, Invercargill, New Zealand (2016) Technical Report. No: 2016/3. Invercargill, New Zealand.

Samberg, L.H., Gerber, J.S., Ramankutty, N., Herrero, M., & West, P.C. (2016). Subnational distribution of average farm size and smallholder contributions to global food production. *Environmental Research Letters*, 11(12): 124010.

Sayre, R., Dangermond, J., Frye, C., Vaughan, R., Aniello, P., Breyer, S., Cribbs, D., Hopkins, D., Nauman, R., Derrenbacher, W. & Wright, D. (2014). A new map of global ecological land units—an ecophysiographic stratification approach. *Washington, DC: Association of American Geographers*, 46.

Scalenghe, R., Edwards, A.C., Barberis, E. & Ajmone Marsan, F. (2010). The influence of pulsed redox conditions on soil phosphorus. *Biogeosciences Discussions*, 7(6), pp.9009-9037.

Schmidt, M. & Lipson, H. (2009). Symbolic regression of implicit equations. *Genetic Programming Theory and Practice*. https://doi.org/doi:https://doi.org/10.1007/978-1-4419-1626-6_5.

Schmidt, M. & Lipson, H. (2015). Eureqa (Version 1.24. 0).

Shiels, D.R. (2010). Implementing landscape indices to predict stream water quality in an agricultural setting: An assessment of the Lake and River Enhancement (LARE) protocol in the Mississinewa River watershed, East-Central Indiana. *Ecological Indicators*, 10(6), pp.1102-1110.

Sivakumar, B. (2004). Dominant processes concept in hydrology: Moving forward. *Hydrological Processes*. https://doi.org/10.1002/hyp.5606.

Sivakumar, B. (2008). Dominant processes concept, model simplification and classification framework in catchment hydrology. *Stochastic Environmental Research and Risk Assessment*, 22(6), 737–748. https://doi.org/10.1007/s00477-007-0183-5.

Snelder, T.H., & Biggs, B.J. (2002). Multiscale river environment classification for water resources management 1. *Journal of the American Water Resources Association*, 38: 1225-1239.

Snelder, T.H., Biggs, B.J.F., & Woods, R.A. (2005). Improved eco-hydrological classification of rivers. *River Research and Applications*, 21(6): 609-628.

StatsNZ. (2018). Agricultural Production Census: Farms by farm count 2017. https://www.stats.govt.nz/information-releases/agricultural-production-statistics-june-2017-final.

Stijven, S., Minnebo, W. & Vladislavleva, K. (2011). Separating the wheat from the chaff: on feature selection and feature importance in regression random forests and symbolic

ESSOAr | https://doi.org/10.1002/essoar.10507536.1 | CC_BY_4.0 | This content has not been peer reviewed.

regression. In Proceedings of the 13th annual conference companion on Genetic and evolutionary computation (pp. 623-630).

Swales, A., Gibbs, M., Olsen, G., & Ovenden, R. (2015). Historical changes in sources of catchment sediment accumulating in Whangarei Harbour, (April), 39. NIWA Client Report No: HAM2015-037

Tratnyek, P. G., Grundl, T. J., & Haderlein, S.B. (Eds). (2012). Aquatic Redox Chemistry. American Chemical Society symposium series 1071; Oxford University Press, 20

Troy, T.J., Wood, E.F., & Sheffield, J. (2008). An efficient calibration method for continental-scale land surface modeling. *Water Resources Research*, 44(9).

Westerhoff, R., White, P., & Miguez-Macho, G. (2018). Application of an improved global-scale groundwater model for water table estimation across New Zealand. *Hydrology and Earth System Sciences*, 22(12): 6449-6472.

Whigham, P.A. & Crapper, P.F. (2001). Modelling rainfall-runoff using genetic programming. *Mathematical and Computer Modelling*, 33(6-7), pp.707-721.

Wilson, S., Chanut, P., Rissmann, C. & Ledgard, G. (2014). Estimating Time Lags for Nitrate Response in Shallow Southland Groundwater. Environment Southland, Invercargill, New Zealand (2014) Technical Report. No: 2014-03.

Wilson, S. R., Close, M. E., & Abraham, P. (2018). Applying linear discriminant analysis to predict groundwater redox conditions conducive to denitrification. Christchurch, New Zealand. *Journal of Hydrology*, 556: 611-624. https://doi:10.1016/j.jhydrol.2017.11.045

Wilson, S.R., Close, M.E., Abraham, P., Sarris, T.S., Banasiak, L., Stenger, R. & Hadfield, J., (2020). Achieving unbiased predictions of national-scale groundwater redox conditions via data oversampling and statistical learning. *Science of the Total Environment*, 705, p.135877.

Wright, R. F. (1988). Influence of Acid Rain on Weathering Rates. In: A. Lerman, & M. Meybeck, Physical and Chemical Weathering in Geochemical Cycles p.181-196. Oslo, Norway: Kluwer Academic Publishers.

ESSOAr | https://doi.org/10.1002/essoar.10507536.1 | CC_BY_4.0 | This content has not been peer reviewed.

Biogeosciences

Supporting Information for

A hydrochemically guided landscape-based classification for water quality: a case study application of process-attribute mapping (PoAM) at a national scale

Clinton W.F. Rissmann[1,2], Lisa K. Pearson[1], Adam P. Martin[3], Matthew I. Leybourne[4], W. Troy Baisden[5], Timothy J. Clough[6], Richard W. McDowell[7], and Jenny G. Webster-Brown[7]

[1] Land and Water Science, 90 Layard Street, Invercargill 9810, New Zealand.

[2] Waterways Centre for Freshwater Management, University of Canterbury and Lincoln University, Private Bag 4800, Christchurch 8140, New Zealand.

[3] GNS Science, Private Bag 1930, Dunedin 9054, New Zealand.

[4] Queen's Facility for Isotope Research, Department of Geological Sciences and Geological Engineering, and Arthur B. McDonald Canadian Astroparticle Physics Research Institute, Department of Physics, Engineering Physics & Astronomy, Queens University, Kingston, Ontario, Canada.

[5] University of Waikato, Private Bag 3105, Hamilton 3240, New Zealand.

[6] Lincoln University, PO Box 85084, Lincoln 7647, New Zealand.

[7] National Science Challenge, AgResearch, Lincoln Science Centre, Private Bag 4749, Christchurch 8140, New Zealand.

Contents of this file

Introduction

Supporting Information 1 provides an extended description of the PoAM method steps and process-attribute gradient hypotheses. Two examples are provided of method application for an atmospheric process-attribute gradient in S2 and classifying reduction potential of the geological material in S3. Supporting Information 4 and 5 presents extended results for the Hybrid Deterministic Genetic Programming modelling. The hydrochemical model response

ESSOAr | https://doi.org/10.1002/essoar.10507536.1 | CC_BY_4.0 | This content has not been peer reviewed.

tables are summarized in S4, and the water quality model response tables are summarized in S5.

S1. PoAM conceptual framework and general methodology

The steps in the PoAM classification and water quality modelling approach (**Fig. 1**) are described in more detail below.

Step 1: Spatial hydrochemical exploration for hypothesis development: Hypothesis development includes specification of the relative sensitivity (importance) and magnitude (direction) of the response of a hydrochemical signature with respect to one or more landscape attribute gradients and is supported by local knowledge of those gradients, relevant literature and/or through the inclusion of existing controlling factor classifications (**Table S1.1**; e.g., Beyer et al., 2016b; Rissmann et al., 2016a; 2019; Snelder and Biggs, 2002; Baisden et al., 2016). In practice, hydrochemical and water quality measures are imported into a GIS and provide the reference point for association with pre-existing spatial classifications of soil, geology and hydrological representations of river and aquifer networks. Multivariate methods, such as principal component analysis, are useful for refining the relative sensitivity of landscape attributes with regards to the spatial variation in hydrochemical signatures (Beyer et al., 2016b; Güler et al., 2002; Rissmann et al., 2018a; b; c; Rodway et al., 2016).

Step 2: Process-attribute gradient map construction: The controlling landscape attributes identified during Step 1 are extracted from one or more existing GIS datasets and combined to replicate, as accurately as possible, gradients for each dominant process (**Table S1.2**). If an important controlling factor is not represented by existing classifications, e.g., the tendency of clay (smectite)-rich soils to crack in response to soil moisture deficit, it may be necessary to generate a representation by extracting and combining relevant controlling factor information (e.g., Beyer et al., 2016b). Historical groundwater quality measures, which often occur at higher spatial densities, are used to guide the editing of geospatial layers so that they represent as faithfully as possible actual process-attribute gradients (Beyer et al., 2016a; Beyer et al., 2016b; Rissmann et al., 2016b; 2018a; b; c). For example, historical measures of electrical conductivity and NO_3^- from unconfined aquifers may be used to refine the effective hydrological boundary, i.e., solute gradient, that exists between a riparian aquifer recharged by an alpine stream and an adjacent lowland aquifer recharged by local precipitation (Beyer et al., 2016b).

Step 3: Process-attribute gradient classification: Grouping of landscape attributes into effective classes is data-driven, using hydrochemical and/or many low-resolution groundwater quality measures (e.g., conductivity; Beyer et al., 2016a; Beyer et al., 2016b; Rissmann et al., 2018a; b; c; **See S2** and **S3**). HCA combined with post hoc significance testing of resultant classes is used for grouping the landscape attributes per hydrochemical measures (Beyer et al., 2016a; Beyer et al., 2016b; Rissmann et al., 2018b; c; Rodway et al., 2016). Given the objective is to represent only the effective attributes of the landscape, the native complexity of existing classifications of landscape attributes are often reduced (Rissmann, 2011; Rissmann et al., 2016a; b; 2018b; c). For example, a regional geological survey data set containing 100 or more individual rock types may be reduced to 3 or 4 main classes per the relative abundance of bioavailable electron donors observed to drive redox succession in shallow aquifer systems (Beyer et al., 2016a; Rissmann et al., 2018b; c). Despite the reduction in the complexity of native classifications, a lack of hydrochemical or water quality data may necessitate a subjective, albeit expert, hydrochemical grouping of attributes (Rissmann et al., 2018c). Resultant classes are subsequently ranked per process signals, and numeric scores assigned. For example, HCA derived clusters defining macro-scale recharge domains are ranked in terms of most- to least-dilute, and highest to lowest -

recharge altitude, according to the concentration of Na, Cl, Br and the stable isotopes of water (Beyer et al., 2016b; Rissmann et al., 2018b; c). Furthermore, mesoscale soil and rock acid neutralizing capacity are ranked from least to most neutralizing according to pH and alkalinity (Rissmann et al., 2018c) and macroscale geological reduction potential of unconfined aquifer systems ranked from most oxidizing to most reducing according to the concentration of redox-sensitive species (Beyer et al., 2016b; Rissmann et al., 2018b; c; Supplementary Materials B). The input data for model development and evaluation is compiled from the process-attribute gradients classification in GIS. Capture zones are generated for the long-term surface water monitoring sites and used to calculate mean scores for each process-attribute gradient, before being exported in a tabular format (Rissmann et al., 2018b; c). Mean process-attribute gradient scores and median hydrochemical data for each site are subsequently log-transformed and Z-scored before correlation analysis and model development and evaluation.

Step 4: Model development and evaluation: This step assesses if the classed process-attribute gradients respond as hypothesized (Step 1) and whether they are sufficiently representative of actual atmospheric, hydrological, redox, and weathering gradients (Rissmann et al., 2018c). Tabulated data is imported into the machine intelligence software package Eureqa (version 1.24.0; Schmidt and Lipson, 2015), which employs a Hybrid Deterministic Genetic Programming (HDGP) approach. Here, HDGP uses the process-attribute gradients as predictors and a process-specific hydrochemical tracer as the target value. HDGP retains those equations that best model the relationship between one or more process-attribute gradient and the process specific tracer, abandoning unpromising solutions (Khu et al., 2001; Schmidt and Lipson, 2009). Specifically, if a process-attribute gradient offers little explanatory power over the spatial variation in a process tracer relative to others, it is automatically excluded during the evolutionary process. After numerous iterations, HDGP converges on a model (i.e., explicit mathematical function) that explains the spatial variation in a dominant process tracer as a function of one or more process-attribute gradients. Model outputs include numeric scores of the sensitivity and magnitude of response and form the basis for testing the hypotheses formulated in Step 1, as well as for evaluating the adequacy with which process-attribute gradients are replicated. The sensitivity of a given process-attribute gradient is defined per its relative impact over a hydrochemical tracer of a dominant process. A positive magnitude occurs when increases in a process-attribute gradient score led to increases in the target variable and vice-versa for a negative magnitude.

Model complexity and accuracy is assessed by the goodness of fit (R^2), correlation coefficient (r), root mean squared error (RMSE) and mean absolute error (MAE) methods (Dubčáková, 2011; Schmidt and Lipson, 2009; Schmidt and Lipson, 2015). Model selection is guided by the trade-off between R^2 and model simplicity, where the R^2 and MAE are analogues to the Akaike information criteria (Aho et al., 2014). Only models that are consistent with the hypotheses for the dominant processes (Step 1) and are relatively accurate (i.e., a cross-validated $R^2 \geq 0.60$) are the mapped process attribute gradients considered fit to be combined with a land use intensity gradient for the estimation of spatial variation in steady-state surface water quality. If the combination of process-attribute gradient maps with land use intensity provides a reasonable estimate of spatial variation in water quality, the model is then considered appropriate for estimation of steady-state surface water quality across data poor areas (Rissmann et al., 2019).

Table S1.1 High-level process-attribute gradient hypotheses.

Dominant Process	Narrative	Most sensitive PAG	Magnitude of response
Atmospheric and hydrological (macroscale) - water source and network routing	Spatial variation in the indicators of precipitation source and hydrological connectivity, i.e., the conservative hydrological tracers Cl and Br will be explained best by the combination of the macro-scale precipitation source (O18), precipitation volume (PPT) and hydrological connectivity (RCD) process-attribute gradients. Other process-attribute gradients will only be retained where the atmospheric and topographic range is subdued.	Macroscale precipitation source, precipitation volume and recharge domain	Cl, Br will exhibit a positive magnitude across the macroscale atmospheric and hydrological process-attribute gradients.
Hydrological pathway (mesoscale)	Spatial variation in K, an indicator of surficial and artificial drainage mediated flow paths, will be explained best by the combination of mesoscale soil hydrological and macroscale precipitation source (18O) process-attribute gradients. (For regions dominated by well-drained soils, lithological (i.e., BGC, SGC and GANC) and geothermal (GTH) process-attribute gradients will be important predictors of K).	Mesoscale hydrological pathway > macroscale atmospheric	K will exhibit a positive magnitude across the mesoscale artificial drainage and macroscale precipitation source process-attribute gradients. In regions without a significant area of imperfectly to poorly drained soils, the magnitude of response of K will be controlled by other process-attribute gradients.
Redox	Spatial variation in redox the indicators FeII and DOC will be explained best by the combination of macroscale atmospheric (18O, PPT), macroscale hydrological connectivity (RCD), mesoscale soil and geological redox potential (SRP, GRP), mesoscale soil hydrological (DD, ART, NBP) and water table (EWT) process-attribute gradients. Lithological process-attribute gradients will be retained as less sensitive predictors.	Atmospheric/ Hydrological = Redox >> lithological	FeII and DOC will exhibit a positive magnitude across the mesoscale redox process-attribute gradients; FeII and DOC will exhibit a positive magnitude across the macroscale atmospheric and hydrological process-attribute gradients; FeII and DOC will exhibit a positive magnitude across the artificial drainage mesoscale soil hydrological process-attribute gradients.
Weathering (chemical)	Spatial variation in the indicators of chemical weathering, i.e., total alkalinity, Ca and $SiO_{2(aq)}$ will be explained best by a combination of mesoscale acid neutralisation capacity (SANC, GANC), regolith cohesion status (SGC and BGC) and macroscale atmospheric (O18, PPT) and hydrological (RCD) process-attribute gradients. (For geothermally active areas, the geothermal (GTH) process-attribute gradients will be an important predictor).	Weathering ≥Hydrological (macro and meso)/Atmospheric	Total alkalinity and Ca will exhibit a positive magnitude across the mesoscale acid neutralisation, macroscale atmospheric and hydrological process-attribute gradients. $SiO_{2(aq)}$ will exhibit a positive magnitude across the mesoscale regolith cohesion status process-attribute gradients.
Weathering (physical)	Spatial variation in the indicators of physical weathering, i.e., black disc clarity will be explained best by combination of macroscale atmospheric (O18, PPT), macroscale hydrological (RCD), mesoscale hydrological pathway (ART, OLF, OLF_DL, DD), mesoscale regolith consolidation status (SGC and BGC), acid neutralisation capacity (SANC and GANC) and soil (SRP) and geological (GRP) reduction potential process-attribute layers. The greater number of sensitive predictors is likely to reflect the complexity of sediment generation and transport dynamics across regions with different climatic and geological histories.	Atmospheric /Hydrological (macro and meso) = Physical and Chemical weathering	Clarity will exhibit a negative magnitude across the macroscale atmospheric and hydrological process-attribute gradients. Clarity will exhibit a positive magnitude across the mesoscale overland flow (OLF) process-attribute gradient; clarity will exhibit a negative magnitude across the mesoscale overland flow of developed land (OLF_DL) process-attribute gradient. The magnitude of response of turbidity and clarity to regolith cohesion status, acid neutralisation and soil and geological redox potential process-attribute gradients will vary between regions according to climatic and geological histories.

N.B. where a region is characterized by a distinct geological (e.g., geothermal activity) or climatic history (e.g., no history of glaciation), variation in the sensitivity and magnitude of process-attribute response gradients is expected. The drivers of regional-scale variation are discussed within the text and acronyms are defined in **Table 2**.

Table S1.2 High-level summary of process-attribute gradients.

Process	Process-Attribute Gradients	Process Tracers	Purpose	Controlling Landscape Attributes	Gradient Type
Atmospheric	Precipitation Source oxygen-18 isoscape ($\delta^{18}O$-H_2O, V-SMOW) (18O) Mean annual precipitation volume (PPT)	Cl, Br	Representation of macroscale precipitation source and volume gradients - prior to routing by the hydrological network.	Altitude and distance from the coast from topography.	Continuous (can also be classed)
Hydrological	Macroscale physiographic recharge domain (RCD), including between domain hydrological connectivity Mesoscale overland flow (OLF), deep drainage (DD), lateral drainage (LAT), natural soil bypass (NBP), artificial drainage (ART), soil slaking and dispersion (HYD); equilibrium water table (EWT)	Na, Cl, Br, SO_4, DOC, K, SiO_2, Total Alkalinity, DO, MnII, FeII, Turbidity (NTU), Clarity (black disk)	Representation of gradients in macroscale recharge source and hydrological routing between domains; representation of mesoscale hydrological pathway (i.e., overland flow, lateral flow, artificial subsurface drainage, soil zone macropore bypass associated with cracking soils, soil slaking and dispersion), and; water table.	Macroscale recharge domains (e.g., alpine, hill, lowland) and connectivity associated with hydrologically connected floodplains both recent (Q2-4) and modern-day (Q1) from topography and geological survey. Mesoscale soil hydrological pathways, occurring within each macroscale recharge domain, are derived from soil survey. Mesoscale water table.	Classed topography, classed soil geological polygons, unclassed water table.
Microbially-mediated Redox	Soil reduction potential (SRP) Geological aquifer reduction potential (GRP)	MnII, FeII, DOC	Representation of gradients in low temperature (< 35 °C), redox succession in unsaturated zone (soil) and saturated zone (aquifer) materials. Note target of aquifer reduction potential is the zone of seasonal water table fluctuation associated with unconfined systems. Dissolved oxygen is a poor tracer of capture zone redox potential in surface waters due to the influence of atmospheric pressure, physical aeration, and in-stream processes.	Soil drainage class and soil organic carbon class from soil survey. Electron donor abundance of aquifer geology from geological class and attendant descriptors (e.g., variably glauconitic limestone, peat in overbank deposits of modern-day floodplains).	Classed soil and geological polygons
Chemical Weathering	Soil acid neutralization capacity (SANC) Geological acid neutralization capacity (GANC)	Total alkalinity, HCO_3, CO_3, dissolved Ca, SiO_2	Representation of gradients in the acid neutralization capacity (ANC) and associated Lewis Base concentration of unsaturated zone and saturated zone materials.	Estimated Lewis base concentration of soil from soil pH, cation exchange capacity, and soil parent material class - soil and geological survey. Lewis base concentration and kinetic dissolution rates of rock and sediment of outcrop, basal layer or aquifer from geological class and attendant descriptors (e.g., shell beds, quartz gravels, ophiolite).	Classed soil and geological polygons
Physical Weathering	Surface cohesion and rock strength (SGC) Basal cohesion and rock strength (BGC)	Turbidity, clarity (black disk)	Representation of gradients in regolith cohesion status and strength that influence mass wasting and erosion processes.	Regolith cohesion status and associated strength as defined by sediment type, cementation status (weakly, moderately, strongly), cement type (carbonate, silicate, oxides/oxy hydroxides) from soil and geological survey.	Classed soil and geological polygons

NTU: Nephelometric Turbidity Unit; DOC: Dissolved Organic Carbon; DO: Dissolved Oxygen.

S2. Example development of the Atmospheric Process-Attribute Gradient

High-level water source hypothesis: The source of water in a stream can be estimated as a function of precipitation source, physiographic recharge domain (e.g., alpine, hill, lowland) and the surface water hydrological network (Baisden et al., 2016; Clark and Fritz, 1997; Kendall and McDonnell, 2012; Rissmann et al., 2019).

Precipitation source, specific hypothesis: Marine aerosol rainout, both wet and dry deposition, is primarily driven by orographic processes.

i. the Cl and Br concentration of surface waters will decrease and increase as altitude and distance from the coast increase and decrease, respectively.

ii. the source of precipitation in a stream, including its recharge altitude, can be reliably estimated as a function of the national precipitation ^{18}O-H_2O (‰, V-SMOW) isoscape layer of Baisden et al. (2016).

Objective: Assess the suitability of the national scale ^{18}O-H_2O precipitation isoscape of New Zealand as a predictor of orographic controls over precipitation source and associated recharge altitude for surface water monitoring sites nationally.

Classification Target: Surface and shallow hydrologically connected groundwaters with a mean age less than c. 100 years old.

Method: A total of 2,061 surface water samples from 687 surface water sites across Northland, Auckland, Waikato, Bay of Plenty, Manawatu, Canterbury, and Southland regions were collated. Three samples, one each under low flow (summer), median flow and event flow (> 75 % of median flow) were collected and an extended hydrochemical suite analysed (**Fig. 2, Table 1**). The three hydrochemical samples were combined with available historical hydrochemical data for the 2007 – 2017 period and median values calculated.

Capture zones for each surface water-monitoring site were generated and the mean, minimum, maximum and range of altitude, relative to mean sea level, were calculated from a digital elevation model (DEM). A raster defining the distance from the coast was then developed from the composite DEM and the mean, minimum, maximum and the range in kilometers was calculated for each of the 687 capture zones and associated surface water-monitoring sites (**Fig. 2**). Mean, minimum, maximum and the range of ^{18}O-H_2O (‰, V-SMOW) in precipitation from the national scale isoscape layer was also calculated (**Fig. 2**). Altitude, distance from the coast and ^{18}O-H_2O of precipitation were then spatially joined to the hydrochemical measures for the 687 surface water monitoring sites with hydrochemical data. A constant was added to all data to remove negative and zero values prior to log10 transformation and z-scoring.

Correlation between the conservative hydrochemical tracers, Cl, Br and landscape attributes were then assessed using the three most commonly used correlation coefficients (i.e., Pearson Product Moment, Spearman Rank, Kendall) and two-tailed probability values at a significance level of 0.05. Overall, altitude was more strongly correlated with Cl and Br concentrations (**Fig. S2.1**) than the distance from the coast. Of the statistical measures of altitude and distance from the coast, mean values were most strongly correlated with Cl and Br concentrations and all were statistically significant (**Fig. S2.1**). For this reason, mean altitude and distance values were used for subsequent analysis.

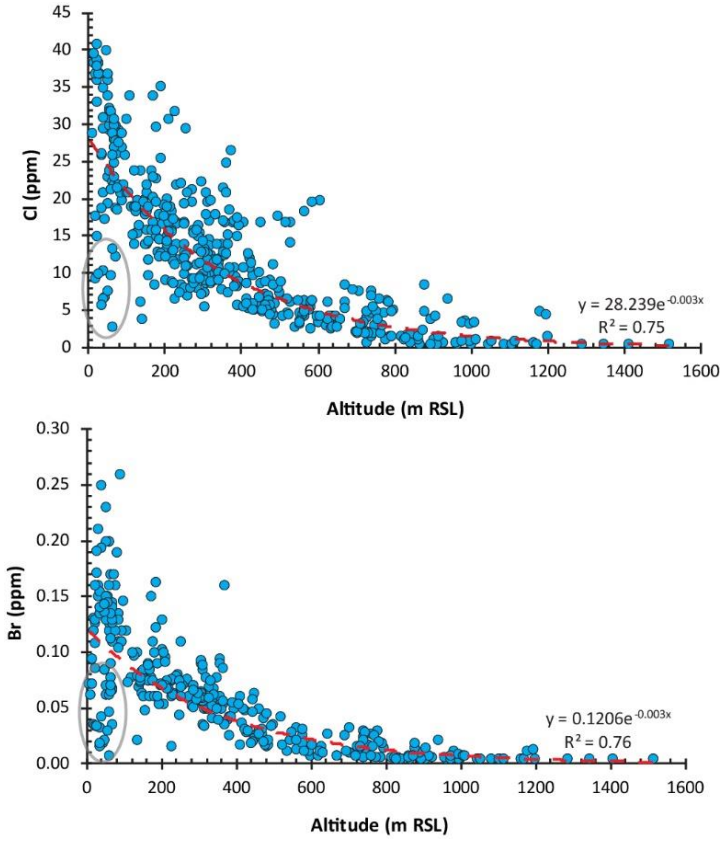

Figure S2.1. Mean altitude versus the median concentration of conservative hydrological tracers Cl and Br in surface waters across 687 sites nationally. Grey ellipses correspond to spring feed streams that discharge at the coast but derive recharge from higher altitude areas. RSL: relative to sea level.

Plots of mean landscape attributes, altitude and distance from the coast are consistent with the rainout of marine aerosols with increasing altitude and/or distance from the coast (Nichol et al., 1997). Importantly, land use derived Cl and Br concentrations are minor relative to the far greater mass of marine aerosol inputs (Nichol et al., 1997; Rissmann et al., 2016a). Further, road de-icing salts that may locally shift halide concentrations in surface and shallow ground water (e.g. Panno et al., 2002) are not extensively used in New Zealand.

To eliminate the influence of collinearity and better understand the dimensional controls over Cl and Br concentrations in streams, principal component analysis was applied to the log transformed and z-scored data following the recommendations of Güler et al. (2002) for hydrochemical data (**Table S2.1**). Principal component analysis revealed a single significant Eigenvalue, lambda ≥ 1.0, that explains 84 % of the variance in the data. Principal component 1 (PC1) indicates a strong correlation and opposite weightings between landscape attributes, mean altitude and distance, and both Cl and Br concentrations, again supporting a strong relationship between the landscape attributes and hydrological tracers of precipitation source.

Table S2.1 Principal component (PC) analysis for altitude (m RSL), distance from the coast and the conservative hydrological tracers Cl and Br.

Component	Eigenvalue	Percent (%)	Cumulative %
1	3.36	0.84	0.84
2	0.40	0.10	0.94
3	0.17	0.04	0.98
4	0.07	0.02	1.00
	PC1	PC2	PC3
Altitude (m RSL)	-0.51	0.21	0.81
Distance from coast (km)	-0.47	0.73	-0.49
Cl	0.52	0.33	0.06
Br	0.50	0.56	0.30

m RSL: meters relative to sea level.

Plots between $\delta^{18}O\text{-}H_2O$ and both Cl (**Fig. S2.2**) and Br were used to evaluate $\delta^{18}O\text{-}H_2O$ of the precipitation layer as an estimator of water source. A clear correlation and distinct regional pattern discriminate between alpine, hill and lowland waters (**Fig. S2.2**). A mixing continuum (dashed lines on **Fig. S2.2**) between hydrologically connected recharge domains can be seen in the data. The relationship is exponential and has commonly been described (Clark and Fritz, 1997; Rissmann et al., 2016a). Also evident is that $\delta^{18}O\text{-}H_2O$ provides additional value through discriminating between southern and northern catchments (**Fig. S2.2**) due to its sensitivity to both longitude and latitude, in addition to altitude (Clark and Fritz, 1997; Kendall and McDonnell, 2012).

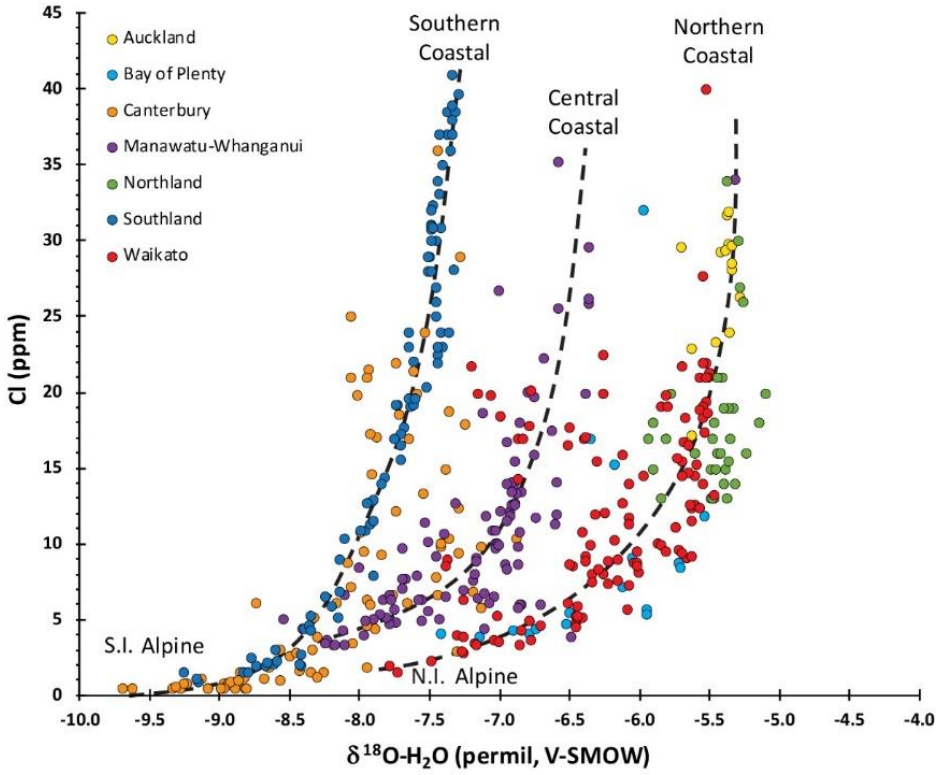

Figure S2.2. The $\delta^{18}O\text{-}H_2O$ of precipitation from the national isoscape layer of Baisden et al. (2016) and median Cl^- concentration for 687 sites nationally. S.I. Alpine: South Island; N.I.: North Island alpine sourced endmembers. Red lines define a mixing continuum where alpine,

hill and/or lowland physiographic domains are hydrologically connected. Note the shift from more negative to positive $\delta^{18}O\text{-}H_2O$ with longitude (south to north).

$\delta^{18}O\text{-}H_2O$ values plotted against mean altitude for the capture zones of each monitoring site, show strong, quantifiable relationships (**Fig. S2.3**). Specifically, linear mixing trajectories across high and low altitude sites are evident. A similar pattern is observed for $\delta^{18}O\text{-}H_2O$ and distance from the coast. Accordingly, the national scale $\delta^{18}O\text{-}H_2O$ precipitation isoscape layer is considered a useful process-attribute gradient for replicating steady-state atmospheric orographic processes over precipitation source and composition prior to its redistribution by the hydrological network.

The results of statistical modelling support the utility of the $\delta^{18}O\text{-}H_2O$ process-attribute gradient, retaining it as the most sensitive predictor of Cl, Br, specific conductivity, and Na across the seven regions with hydrochemical data **(**see **S4)**. These findings are consistent with those reported by Rissmann et al. (2019), who collected and measured $\delta^{18}O\text{-}H_2O$ (V-SMOW), Cl and Br in precipitation across Southland, New Zealand. These authors evaluated the relationship between Cl, Br and $\delta^{18}O\text{-}H_2O$ in precipitation and both recharge altitude and distance from the coast, revealing a strong exponential relationship that was then used to generate a regional precipitation source process-attribute gradient layer. The resultant layer was then used to support the estimation of recharge source and associated recharge altitude for surface waters across the Southland region.

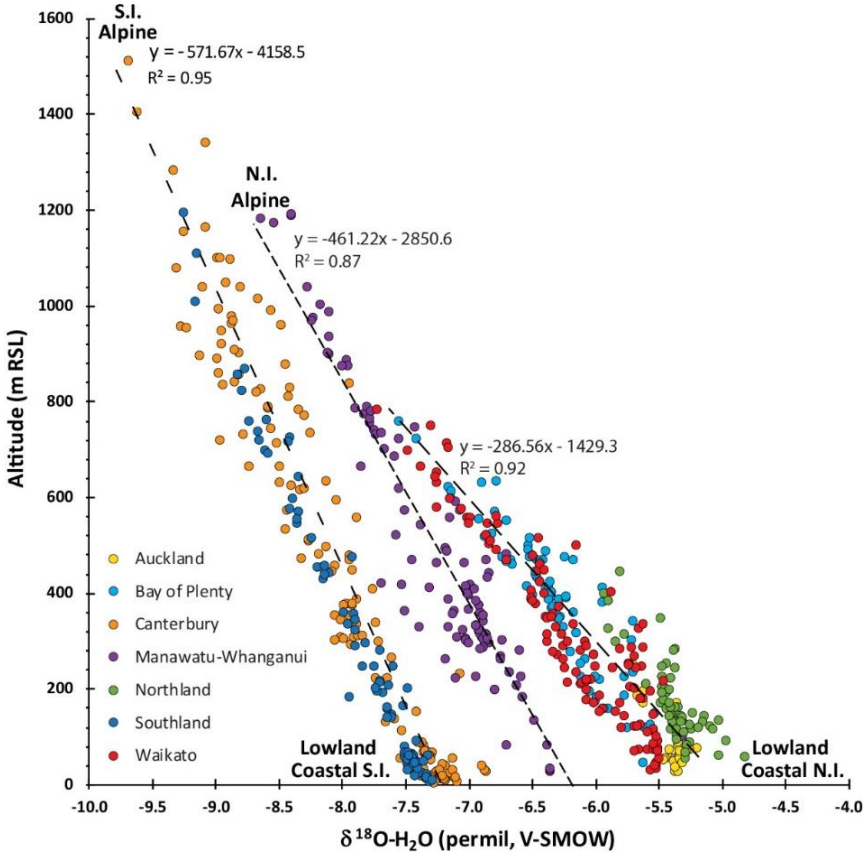

Figure S2.3. The $\delta^{18}O\text{-}H_2O$ of precipitation from the national isoscape layer of Baisden et al. (2016) and mean catchment altitude for 687 sites nationally. Note the ability to estimate mean recharge altitude and the discrimination of monitoring sites according to longitude. S.I.: South Island; N.I.: North Island; RSL: relative to sea level.

The above defines the manual component for evaluating the utility of the national scale $\delta^{18}O\text{-}H_2O$ precipitation isoscape of Baisden et al. (2016). The resultant process-attribute gradient is used as a representation of the steady-state atmospheric orographic gradient governing precipitation source (chemical and isotopic composition) prior to redistribution by the hydrological network (**Fig. S2.4**). The main caveat of the precipitation source process-attribute gradient is that it is not a standalone layer and should not be used that way. Rather, it should be used in combination with other process-attribute gradients, such as the recharge domain (i.e., alpine, hill, mixed and lowland) process-attribute gradient to estimate the source and proportional mixing of water at any point along the surface water hydrological network.

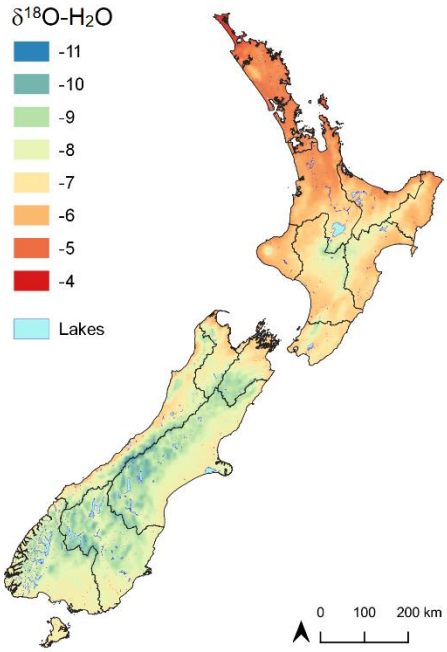

Figure S2.4. The $\delta^{18}O\text{-}H_2O$ (V-SMOW) of precipitation process attribute gradient from the national isoscape layer of Baisden et al. (2016).

S3. Example development of the Aquifer Reduction Potential Process-Attribute Gradient

High-level redox potential hypothesis: Redox potential relevant to the surface water network will vary as a function of soil reduction potential (Rissmann et al., 2016a; Wilson et al., 2018), natural soil bypass where soils crack in response to soil moisture deficit (Kurtzman et al., 2016; Rissmann et al., 2016a; 2019), macroscale hydrological connectivity of the coupled surface-groundwater network (Rissmann et al., 2016a, 2019) and the electron donor abundance of aquifer materials (Krantz and Powars, 2000; McMahon and Chapelle, 2008).

Aquifer reduction potential specific hypothesis: The redox potential of unconfined aquifers is partially controlled by the electron donor abundance of aquifer materials - mainly organic carbon with minor contributions from inorganic electron donors, such as pyrite and glauconite.

Objective: Generate a rubric to classify existing, national-scale geological data in terms of electron donor abundance relevant to the uppermost portion of unconfined aquifers and the shallow surface water network.

Classification target: Uppermost portion of unconfined aquifers, especially the zone of water table fluctuation that drives export to the stream network.

Method: Hydrochemical well data (n: 2,191) with an extended hydrochemical suite was collated from the 7-participating regions. Wells without depth data and those defined as confined and semi-confined were removed from the data set. Wells with depth information but lacking a confinement status were evaluated against the national scale equilibrium water table layer of Westerhoff et al. (2018). For example, if the equilibrium water table is < 1 m below ground level, yet the well is deep, e.g., > 30 m, it may be semi-confined or confined. These wells are flagged to note that their confinement status may not represent the classification target, i.e., the uppermost portion of a confined aquifer. Confinement status screening reduced the data set to 1,215 wells and six regions. Median hydrochemical scores for each analyte were then calculated following quality assurance.

Groundwater redox assignments were generated through the application of HCA to log-transformed and z-scored data following the recommendations of Güler et al. (2002). HCA using Ward's linkage and the Euclidian distance was applied to the most abundant redox-sensitive measures in the groundwater dataset, dissolved oxygen (DO), MnII and FeII (**Fig. S3.1; Table S3.1**). A low observation threshold (phenon line) in the resultant dendrogram was selected to maximise the number of clusters associated with variation in redox-sensitive species. Although not included in the redox assignments, groundwater NO_2-N and NO_3-N (NNN) was chosen as the grouping variable as oxidised nitrogen species are commonly the main anthropogenic groundwater quality contaminant of concern. Using a lower observational threshold allows for clusters to be combined if there is limited evidence that NNN is not significantly different between redox potential clusters.

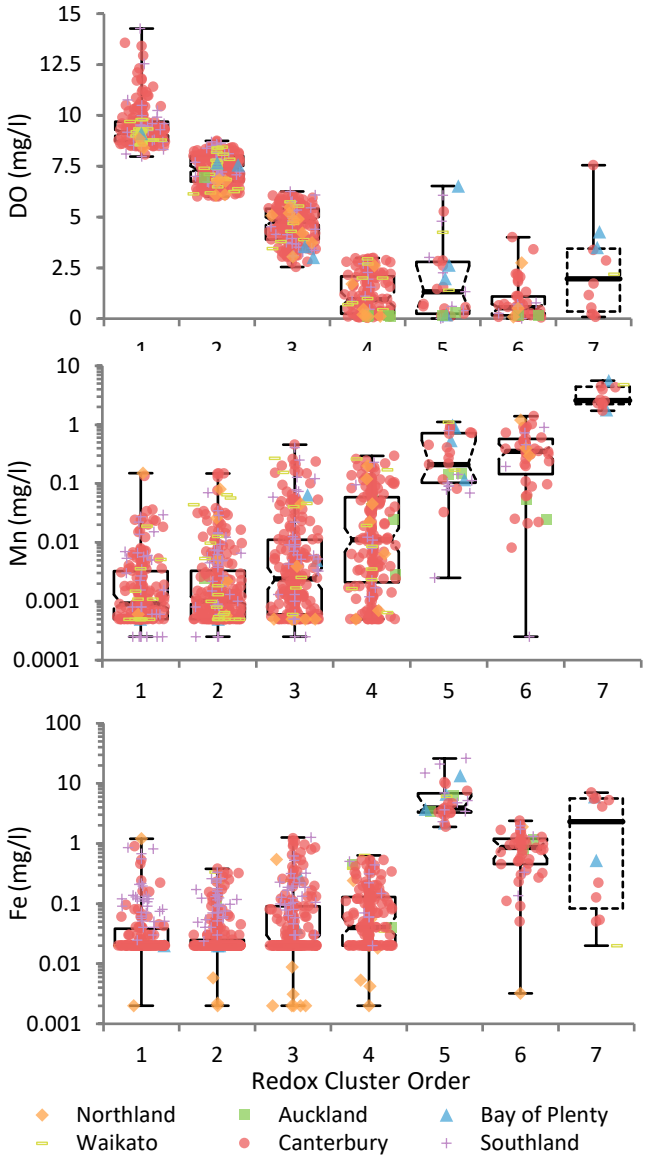

Figure S3.1 Plots of redox potential clusters for dissolved oxygen (DO), MnII and FeII represent a continuum from strongly oxidizing (Cluster 1) to strongly reducing (Cluster 7). See **Table S3.1** for plot details.

Table S3.1 Summary showing the cluster membership number, mean, median and 95% confidence interval for dissolved oxygen (DO), MnII and FeII, dissolved organic carbon (DOC) and nitrate-nitrite nitrogen (NNN). See **Figures S3.1** and **S3.2** for accompanying plots.

Cluster	Measure	N	Mean	Median	95% CI
1	DO	223	9.4	9.2	9.0 - 9.3
2	DO	343	7.3	7.3	7.2 - 7.5
3	DO	261	4.6	4.8	4.6 - 5.0
4	DO	189	1.2	0.9	0.6 - 1.3
5	DO	31	1.8	1.3	0.4 - 2.6
6	DO	48	0.8	0.5	0.3 - 0.7
7	DO	12	2.3	2	0.2 - 3.5
1	Mn	223	0.0046	0.0009	0.0008 - 0.0013
2	Mn	343	0.0061	0.0010	0.0009 - 0.0012
3	Mn	261	0.0228	0.0024	0.0016 - 0.0037
4	Mn	189	0.042	0.011	0.007 - 0.0017
5	Mn	31	0.376	0.210	0.117 - 0.540
6	Mn	48	0.42	0.35	0.26 - 0.47
7	Mn	12	3.22	2.58	2.20 - 4.50
1	Fe	223	0.06	0.02	0.02 - 0.02
2	Fe	343	0.04	0.02	0.02 - 0.02
3	Fe	261	0.11	0.02	0.02 - 0.03
4	Fe	189	0.1	0.04	0.03 - 0.06
5	Fe	31	6.36	3.9	3.40 - 6.11
6	Fe	48	0.9	0.86	0.56 - 1.12
7	Fe	12	2.87	2.31	0.053 - 5.70
1	DOC	78	1.13	0.67	0.54 - 0.84
2	DOC	143	1.17	0.70	0.60 - 0.85
3	DOC	122	1.47	0.80	0.60 - 1.10
4	DOC	32	2.98	1.30	1.00 - 2.30
5	DOC	15	3.24	1.55	1.00 - 4.69
6	DOC	14	2.74	2.53	1.50 - 4.60
7	DOC	5	3.66	3.30	-
1	NNN	219	5.28	4.20	3.10 - 5.00
2	NNN	334	4.74	3.48	2.80 - 4.00
3	NNN	255	3.85	2.90	2.50 - 3.50
4	NNN	187	2.32	0.52	0.29 - 0.85
5	NNN	31	0.73	0.05	0.03 - 0.47
6	NNN	48	1.22	0.06	0.05 - 0.17
7	NNN	12	1.42	0.05	0.00 - 2.45

Dissolved organic carbon (DOC), total alkalinity (generated in response to reduction), total Kjeldahl nitrogen and ammonium were then plotted by redox cluster as a further check of the association between redox potential clusters and other indicators of redox control. Here, DOC is assumed to be an indicator of the abundance of solid-state organic carbon and hence electron donor abundance in the aquifer (**Fig. S3.2; Table S3.1).** Multiple comparisons using the t-distribution method at the 95 % level was used to determine the significance of the 7-redox potential clusters in terms of groundwater NNN (**Fig. S3.2**, **Table S3.1 and S3.2**). Based on multiple comparisons testing, redox potential clusters 5 – 7 were grouped into a single redox group defined as 'Strongly Reducing'. The remaining redox potential clusters were significantly different at the 95 % level. The resulting five homogenous subsets were then assigned a redox category according to DO, MnII and FeII concentrations (**Table S3.2**).

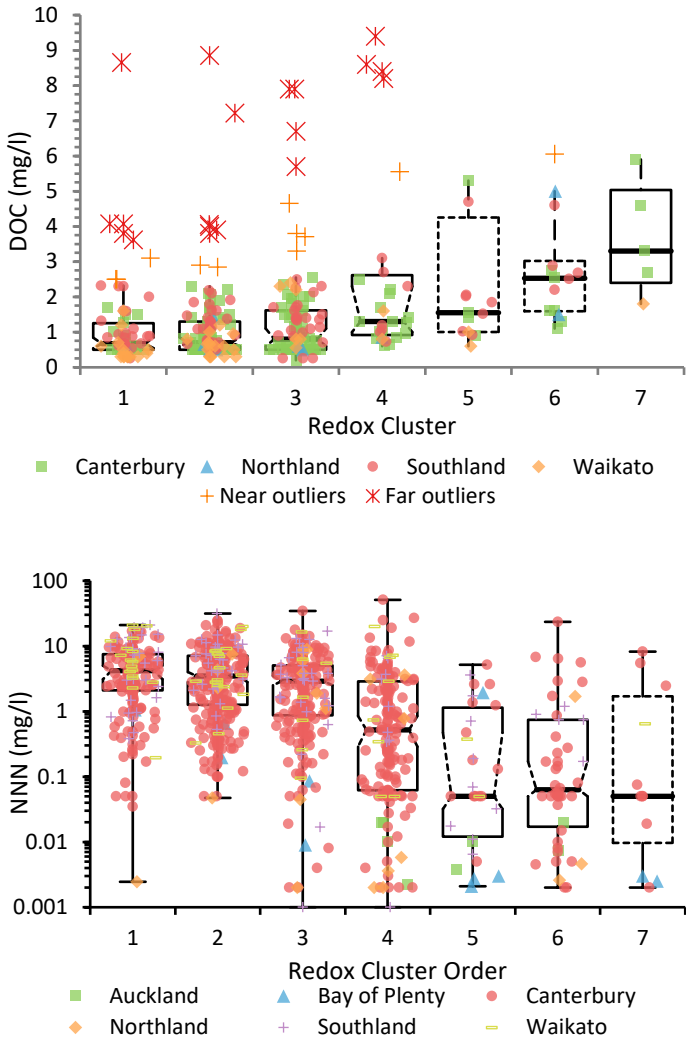

Figure S3.2 Plots of redox potential clusters for dissolved organic carbon (DOC) and nitrate-nitrite nitrogen (NNN). See **Table S3.1** for plot details.

Table S3.2 Summary of redox potential classes.

Group	Redox Cluster	Redox Potential Category
1	1	Strongly oxidising
2	2	Oxidising
3	3	Mixed (oxidising-reducing)
4	4	Reducing
5	5, 6, 7	Strongly reducing

The resultant redox potential classes were then spatially referenced to relevant landscape factors surrounding the well/bore (100 m radius). Specifically, each bore is intersected with the national quarter-million scale geological map of New Zealand (QMAP) for the lithology fields ‘main rock’ and ‘sub-rock’, the stratigraphy fields ‘stratlex’ and ‘geological description’ and the chronology field ‘geomorphic age’ (both minimum and maximum ages), before cross-referencing to bore log descriptions provided by regional authorities. The association between aquifer geology and redox class is then used to generate

five ‘geological reduction potential’ classes as per Krantz and Powars (2000) and Rissmann (2011). The resulting geological reduction potential rubric (**Table S3.3**) was then used to assign a likely geological reduction potential class to the national quarter-million scale geological map using definition queries within a GIS to isolate the association between redox categories and aquifer composition. The resulting geological reduction potential process-attribute gradient (**Fig. S3.3**) exhibits a strong spatial correlation to known groundwater nitrate hotspots nationally (Rissmann, 2011, 2012; Close et al., 2016; Ministry for the Environment and Stats NZ, 2020).

Table S3.3 Geological reduction potential (GRP) rubric for classifying national geological data.

Geological Unit	Geological Composition	Reduction Potential	Class
Active peat wetlands	Peat	High	5
Estuarine sediments	Estuarine sediments	High	5
Low rank coal measures	Lignite, alluvial gravels over lignite	Moderately high	4
Mixed marine-terrestrial terraces	Marine or ocean sediment	Moderate	3
Glauconitic limestone	Limestone with variable glauconite or greensand	Moderate	3
Carbonaceous sediments	Minor carbonaceous sediments (coal or carbon)	Moderate	3
Pyritic sediments	Sediments with variable pyrite	Moderate	3
Mudstones	Mudstone sediments (non-siliceous or argillic, poorly indurated)	Moderate	3
Minor muds	Muds (not mudstone)	Moderately low	2
River floodplains – minor peat	Alluvial gravels, sand, silt, and clay with minor peat	Moderately low	2
Modern river floodplains	Alluvial gravel, sand, silt and clay	Low	1
Terraces/outwash plains/Glacial deposits	Weathered gravel, sand, silt and clay	Low	1
High terrace and basin gravels	Highly weathered gravel, sand, silt and clay	Low	1
Volcanic deposits	Ignimbrite and other volcanic deposits	Low	1

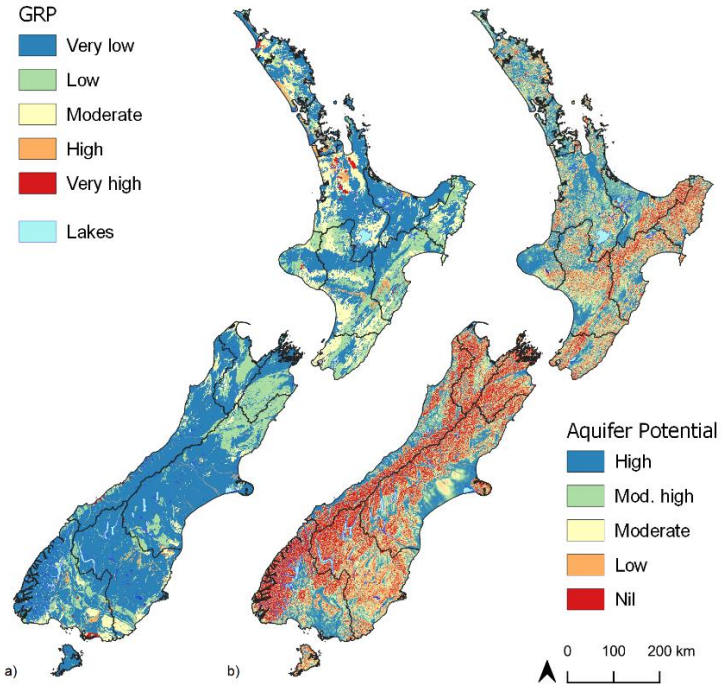

Figure S3.3 a) Geological reduction potential (GRP) process attribute gradient and b) aquifer potential (EWT) as defined by both an unconfined aquifer that is hydrologically connected to the surface water network (modified from the Equilibrium Water Table classification of

Westerhoff et al. (2018). Where the water table is deep, relative to the land surface, aquifer connectivity to stream is limited, and as such aquifer potential is ranked as being lower.

Statistical modelling retained the resultant geological reduction potential and/or the aquifer potential layer as a sensitive predictor of total phosphorus and dissolved reactive phosphorus across most of the country (**see S5**). The geological reduction potential layer was seldom retained as a sensitive predictor of total nitrogen and NNN in surface waters, with the soil reduction potential process-attribute gradient identified as a more sensitive predictor. The significant influence of soil reduction potential over unconfined aquifer and surface water redox potential was identified for the Southland region by Rissmann et al. (2016a) and subsequently by Wilson et al. (2018).

Limitations to the geological reduction potential classification are the horizontal- and depth-resolution of aquifer lithology available from the national geological layer. However, this effect is minimised as the target is the zone of water table fluctuation near-surface. It is worth emphasising that the geological reduction potential process-attribute gradient is not a standalone layer and should not be used as such. Rather, it is to be used in combination with other process attribute gradients, such as soil reduction potential (SRP), soil zone bypass due to shrink-swell soils (NBP), macroscale hydrological connectivity (RCD), and water table depth (EWT) to best define the shallow redox gradients most relevant to the surface water hydrological network. This combined use of process-attribute gradients was undertaken in this study.

S4. Surface Water Hydrochemical Model Response

Table S4.1. Process-attribute gradients retained by models, sensitivities, and the magnitude of response hydrochemical tracers of each dominant process across all 7 regions.

Tracer	PAG	Sensitivity	% Positive	Positive Magnitude	% Negative	Negative Magnitude
Cl	O18	0.79	100	0.79	0	1.23
	PPT	0.75	40	0.44	60	0.96
	RCD	0.04	100	0.04	0	0.00
Br	PPT	0.88	66	0.63	34	1.37
	O18	0.75	100	0.75	0	0.00
	RCD	0.31	100	0.31	0	0.00
K	O18	0.98	100	0.87	0	0.00
	SGC	0.43	0	0.00	100	0.43
	RCD	0.28	98	0.28	2	0.01
	GTH	0.24	100	0.24	0	0.00
	PPT	0.23	0	0.00	100	0.23
	GRP	0.02	0	0.00	100	0.02
FeII	SRP	0.70	100	0.70	0	0.00
	PPT	0.46	61	0.53	39	0.35
	ART	0.19	42	0.15	58	0.21
	O18	0.10	100	0.10	0	0.00
DOC	ART	0.68	90	0.74	10	0.05
	GRP	0.15	100	0.15	0	0.00
	PPT	0.12	85	0.12	15	0.13
	SRP	0.12	99	0.12	1	0.04
	O18	0.06	100	0.06	0	0.00
Total Alkalinity	GANC	0.73	100	0.73	0	0.00
	PPT	0.67	0	0.00	100	0.67
	BGC	0.47	0	0.00	100	0.47
	O18	0.31	100	0.31	0	0.00
	SRP	0.09	0	0.00	100	0.09
Ca	BGC	0.70	8	0.25	92	0.74
	GANC	0.42	100	0.42	0	0.00
	PPT	0.30	0	0.00	100	0.30
	NBP	0.12	100	0.12	0	0.00
	EWT	0.03	100	0.03	0	0.00
	SANC	0.01	63	0.01	37	0.00
$SiO_{2(aq)}$	BGC	0.48	77	0.47	23	0.54
	O18	0.39	100	0.39	0	0.00
	RCD	0.32	100	0.32	0	0.00
	PPT	0.27	0	0.00	100	0.27
	GANC	0.01	100	0.01	0	0.00
Clarity	SGC	0.49	100	0.50	0	0.00
	EWT	0.45	40	0.41	60	0.48
	DD	0.25	100	0.25	0	0.00
	NBP	0.19	100	0.19	0	0.00

DOC: Dissolved organic carbon

Table S4.2. Process-attribute gradients retained by models, sensitivities, and the magnitude of response of hydrological tracers of water source by regional subset.

Analyte	Region	Variable	Sensitivity	% Positive	Positive Magnitude	% Negative	Negative Magnitude
Cl	Northland - Auckland	PPT	1.02	0	0.00	100	1.02
		RCD	0.34	0	0.00	100	0.34
		O18	0.07	31	0.10	69	0.05
		OLF	0.02	0	0.00	100	0.02
	Waikato – Bay of Plenty	O18	0.63	100	0.63	0	0.00
		PPT	0.63	68	0.15	32	1.67
		RCD	0.44	87	0.38	13	0.88
	Manawatu	O18	1.24	98	1.26	2	0.45
		PPT	0.64	20	1.15	80	0.51
		RCD	0.15	88	0.00	12	0.02
	Canterbury	O18	0.99	74	0.99	26	1.01
		RCD	0.30	100	0.30	0	0.00
		PPT	0.27	48	0.29	52	0.24
	Southland	O18	1.37	100	1.37	0	0.00
		PPT	0.22	85	0.22	15	0.25
		RCD	0.17	100	0.17	0	0.00
Br	Northland - Auckland	PPT	0.87	0	0	100	0.87
		RCD	0.29	96	0.29	4	0.14
		O18	0.14	100	0.14	0	0.00
	Manawatu	O18	1.80	99	1.67	1	13.24
		RCD	0.36	100	0.36	0	0.00
		PPT	0.34	5	0.38	95	0.34
	Canterbury	RCD	2.03	94	1.44	6	11.65
		O18	0.38	97	0.40	3	0.02
	Southland	O18	0.57	56	0.66	44	0.45
		RCD	0.47	100	0.47	0	0.00
		PPT	0.14	100	0.14	0	0.00
K	Northland - Auckland	PPT	0.64	25	0.24	75	0.78
		BGC	0.30	0	0.00	100	0.30
		SGC	0.06	100	0.06	0	0.00
		GANC	0.05	100	0.05	0	0.00
		AREA	0.02	0	0.00	100	0.02
		DD	0.01	0	0.00	100	0.01
	Waikato – Bay of Plenty	GTH	0.38	100	0.38	0	0.00
		GANC	0.37	0	0.00	100	0.37
		O18	0.36	100	0.36	0	0.00
		SGC	0.28	0	0.00	100	0.28
		OLF	0.25	0	0.00	100	0.25
		RCD	0.02	100	0.02	0	0.00
	Manawatu	ART	0.47	100	0.47	0	0.00
		O18	0.47	100	0.47	0	0.00
		CEC	0.36	0	0.00	100	0.36
		BGC	0.31	7	0.07	93	0.33
		PPT	0.01	100	0.01	0	0.00
		SGC	0.01	0	0.00	100	0.01
	Canterbury	ART	0.68	100	0.68	0	0.00
		O18	0.46	100	0.46	0	0.00
		$SANC_{pH}$	0.01	73	0.01	27	0.01
	Southland	ART	0.77	100	0.77	0	0.00
		O18	0.42	100	0.42	0	0.00
		NBP	0.30	0	0.00	100	0.30
		DD	0.18	100	0.18	0	0.00

NB. Insufficient Br^- data available for Waikato-Bay of Plenty regions.

Table S4.3. Process-attribute gradients retained by models, sensitivities, and the magnitude of response of redox tracers by regional subset.

Analyte	Region	Variable	Sensitivity	% Positive	Positive Magnitude	% Negative	Negative Magnitude
FeII	Northland - Auckland	DD	0.73	0	0.00	100	0.73
		$SANC_{CEC}$	0.34	85	0.34	15	0.38
		PPT	0.27	100	0.27	0	0.00
		GANC	0.24	0	0.00	100	0.24
		ART	0.23	100	0.23	0	0.00
		OLF	0.07	100	0.07	0	0.00
	Waikato – Bay of Plenty	SRP	0.35	89	0.38	11	0.07
		EWT	0.28	0	0.00	100	0.28
		$SANC_{CEC}$	0.09	100	0.09	0	0.00
		O18	0.05	0	0.00	100	0.05
		PPT	0.04	11	0.01	89	0.04
		RCD	0.03	94	0.03	6	0.00
	Manawatu	O18	0.83	100	0.83	0	0.00
		EWT	0.58	0	0.00	100	0.58
		BGC	0.49	100	0.49	0	0.00
		PPT	0.48	0	0.00	100	0.48
		GANC	0.20	57	0.25	43	0.13
		GRP	0.09	100	0.09	0	0.00
		SRP	0.06	100	0.06	0	0.00
		OLF	0.04	100	0.04	0	0.00
	Canterbury	SGC	5.15	100	5.15	0	0.00
		PPT	1.42	20	0.85	80	1.56
		DD	0.74	0	0.00	100	0.74
		GANC	0.16	70	0.16	30	0.18
	Southland	O18	0.62	100	0.62	0	0.00
		NBP	0.19	0	0.00	100	0.19
		GRP	0.16	100	0.16	0	0.00
		EWT	0.15	100	0.15	0	0.00
		DD	0.15	0	0.00	100	0.15
		$SANC_{pH}$	0.09	2	0.02	98	0.09
		ART	0.04	100	0.04	0	0.00
DOC	Northland - Auckland	GANC	0.98	51	0.79	49	1.17
		SRP	0.62	100	0.62	0	0.00
		HYD	0.56	43	0.58	57	0.54
		ARTD	0.44	100	0.44	0	0.00
		O18	0.37	0	0.00	100	0.37
		SGC	0.13	0	0.00	100	0.13
	Manawatu	PPT	0.84	0	0.00	100	0.84
		EWT	0.66	0	0.00	100	0.66
		$SANC_{CEC}$	0.28	98	0.28	2	0.15
		ART	0.19	0	0.00	100	0.19
		GRP	0.19	86	0.19	14	0.18
		RCD	0.07	0	0.00	100	0.07
	Canterbury	O18	5.73	64	5.98	36	5.28
		PPT	0.73	29	0.49	71	0.83
		NBP	0.65	10	2.42	90	0.46
		EWT	0.34	100	0.34	0	0.00
	Southland	SRP	0.57	85	0.58	15	0.51
		NBP	0.25	0	0.00	100	0.25
		O18	0.16	100	0.16	0	0.00
		ART	0.11	100	0.11	0	0.00
		$SANC_{pH}$	0.07	12	0.02	88	0.08

DOC: Dissolved organic carbon. Insufficient DOC data available for Waikato-BOP regions.

Table S4.4. Process-attribute gradients retained by models, sensitivities, and magnitude of response of chemical weathering tracers by regional subset.

Analyte	Region	Variable	Sensitivity	% Positive	Positive Magnitude	% Negative	Negative Magnitude
Total Alkalinity	Northland - Auckland	O18	0.56	100	0.56	0	0.00
		$SANC_{pH}$	0.32	100	0.32	0	0.00
		GANC	0.28	100	0.28	0	0.00
		SRP	0.21	79	0.23	21	0.13
		PPT	0.09	17	0.13	83	0.08
		BGC	0.01	100	0.01	0	0.00
	Waikato – Bay of Plenty	SGC	0.69	0	0.00	100	0.69
		GANC	0.66	100	0.66	0	0.00
		PPT	0.55	0	0.00	100	0.55
		GTH	0.27	100	0.27	0	0.00
		RCD	0.14	0	0.00	100	0.14
		$SANC_{pH}$	0.14	100	0.14	0	0.00
		BGC	0.07	0	0.00	100	0.07
	Manawatu	BGC	0.63	0	0.00	100	0.63
		GANC	0.47	97	0.48	3	0.07
		RCD	0.35	6	0.20	94	0.36
		PPT	0.18	0	0.00	100	0.18
		SRP	0.01	47	0.01	53	0.01
	Canterbury	O18	0.88	100	0.88	0	0.00
		GRP	0.44	66	0.57	34	0.19
		$SANC_{pH}$	0.32	100	0.32	0	0.00
		GANC	0.22	0	0.00	100	0.22
	Southland	GANC	0.66	100	0.66	0	0.00
		SRP	0.40	79	0.45	21	0.21
		O18	0.38	100	0.38	0	0.00
		PPT	0.31	0	0.00	100	0.31
		$SANC_{pH}$	0.31	99	0.31	1	0.20
Ca	Northland - Auckland	GANC	0.93	52	1.00	48	0.85
		PPT	0.53	0	0.00	100	0.53
		BGC	0.30	17	0.17	83	0.33
		O18	0.26	100	0.26	0	0.00
		EWT	0.25	67	0.28	33	0.18
	Waikato – Bay of Plenty	GANC	0.69	100	0.69	0	0.00
		SGC	0.41	0	0.00	100	0.41
		RCD	0.25	100	0.25	0	0.00
		BGC	0.22	1	0.05	99	0.22
		PPT	0.10	0	0.00	100	0.10
		EWT	0.04	0	0.00	100	0.04
		GTH	0.03	100	0.03	0	0.00
	Manawatu	BGC	0.75	0	0.00	100	0.75
		RCD	0.43	0	0.00	100	0.43
		GANC	0.30	100	0.30	0	0.00
		GRP	0.24	100	0.24	0	0.00
		$SANC_{pH}$	0.18	100	0.18	0	0.00
		SRP	0.04	57	0.05	43	0.04
	Canterbury	PPT	3.37	57	4.18	43	2.29
		O18	1.15	78	1.32	22	0.57
		BGC	0.44	52	0.48	48	0.40
		GANC	0.35	78	0.35	22	0.35
	Southland	ARTD	0.51	100	0.51	0	0.00
		O18	0.34	100	0.00	0	0.50
		OLF_DL	0.22	0	0	100	0.00
		GANC	0.20	100	0.20	0	0.00
		NBP	0.14	100	0.14	0	0.00
		$SANC_{CEC}$	0.12	100	0.12	0	0.00
SiO_2	Northland - Auckland	GRP	0.68	0	0.00	100	0.68
		$SANC_{pH}$	0.48	76	0.54	24	0.29

Analyte	Region	Variable	Sensitivity	% Positive	Positive Magnitude	% Negative	Negative Magnitude
		OLF	0.33	81	0.34	19	0.28
		GANC	0.20	74	0.25	26	0.06
		PPT	0.07	0	0.00	100	0.07
		EWT	0.07	85	0.07	15	0.04
	Waikato – Bay of Plenty	GTH	0.55	100	0.55	0	0.00
		SGC	0.43	100	0.43	0	0.00
		OLF	0.26	0	0.00	100	0.26
		GANC	0.24	0	0.00	100	0.24
		PPT	0.22	0	0.00	100	0.22
		BGC	0.22	100	0.22	0	0.00
	Manawatu	SGC	0.70	100	0.70	0	0.00
		PPT	0.65	0	0.00	100	0.65
		EWT	0.65	0	0.00	100	0.65
		SRP	0.30	0	0.00	100	0.30
		OLF	0.13	1	0.01	99	0.13
		DD	0.13	46	0.14	54	0.12
		BGC	0.09	0	0.00	100	0.09
	Canterbury	RCD	0.76	100	0.76	0	0.00
		BGC	0.59	48	0.53	52	0.64
		SGC	0.51	100	0.51	0	0.00
		$SANC_{pH}$	0.45	99	0.46	1	0.06
		DD	0.10	100	0.10	0	0.00
		GANC	0.00	0	0.00	100	0.00
	Southland	RCD	0.76	100	0.76	0	0.00
		BGC	0.59	48	0.53	52	0.64
		SGC	0.51	100	0.51	0	0.00
		$SANC_{pH}$	0.45	99	0.46	1	0.06
		DD	0.10	100	0.10	0	0.00
		GANC	0.00	0	0.00	100	0.00

Table S4.5. Process-attribute gradients retained by models, sensitivities, and magnitude of response of physical weathering tracers by regional subset.

Analyte	Region	Variable	Sensitivity	% Positive	Positive Magnitude	% Negative	Negative Magnitude
Clarity	Northland - Auckland	SGC	0.76	100	0.76	0	0.00
		SRP	0.54	100	0.54	0	0.00
		DD	0.41	100	0.41	0	0.00
		AREA	0.38	0	0.00	100	0.38
		CEC	0.28	0	0.00	100	0.28
		RCD	0.12	100	0.12	0	0.00
	Waikato – Bay of Plenty	ART	1.35	0	0.00	100	1.35
		SGC	0.34	100	0.34	0	0.00
		SRP	0.31	100	0.31	0	0.00
		OLF_{DL}	0.28	0	0.00	100	0.28
		OLF	0.04	98	0.04	2	0.01
	Manawatu	SRP	1.93	62	1.10	38	3.32
		O18	0.95	15	1.08	85	0.92
		AREA	0.65	0	0.00	100	0.65
		PPT	0.23	100	0.23	0	0.00
		OLF	0.22	27	0.38	73	0.16
	Canterbury	AREA	0.78	100	0.78	0	0.00
		O18	0.71	91	0.71	9	0.68
		HYD	0.70	0	0.00	100	0.70
		OLF_{DL}	0.57	96	0.57	4	0.47
		PPT	0.35	0	0.00	100	0.35
		CEC	0.32	0	0.00	100	0.32
		OLF	0.25	0	0.00	100	0.25
	Southland	O18	0.90	0	0.00	100	0.90
		GANC	0.28	74	0.35	26	0.10
		OLF_{DL}	0.24	0	0.00	100	0.24
		AREA	0.19	0	0.00	100	0.19
		PPT	0.03	0	0.00	100	0.03

ESSOAr | https://doi.org/10.1002/essoar.10507536.1 | CC_BY_4.0 | This content has not been peer reviewed.

S5. Surface Water Quality Model Response and Performance

Table S5.1 Total nitrogen model sensitivities by regional subset.

Region	Variable	Sensitivity	% Positive	Positive Magnitude	% Negative	Negative Magnitude
Northland - Auckland	LUI	0.74	100	0.74	0	0.00
	RCD	0.67	67	0.69	33	0.64
	SRP	0.32	100	0.32	0	0.00
	18O	0.14	0	0.00	100	0.14
Waikato – Bay of Plenty	GTH	1.57	100	1.57	0	0.00
	LUI	0.55	100	0.55	0	0.00
	ART	0.33	100	0.33	0	0.00
	RCD	0.31	100	0.31	0	0.00
	EWT	0.12	0	0.00	100	0.12
	AREA	0.10	0	0.00	100	0.10
	OLF_{DL}	0.06	100	0.06	0	0.00
	$SANC_{CEC}$	0.03	100	0.03	0	0.00
	$SANC_{pH}$	0.03	100	0.03	0	0.00
Wellington-Manawatu-Taranaki	LUM	0.37	100	0.37	0	0.00
	18O	0.29	100	0.29	0	0.00
	BGC	0.24	0	0.00	100	0.24
	GANC	0.16	0	0.00	100	0.16
	ART	0.14	100	0.14	0	0.00
	HYD_{DL}	0.13	100	0.13	0	0.00
	RCD	0.12	100	0.12	0	0.00
	SGC	0.03	100	0.03	0	0.00
Hawkes Bay - Gisborne	LUI	0.82	100	0.82	0	0.00
	RCD	0.37	100	0.37	0	0.00
	NBP	0.27	45	0.15	55	0.38
	$SANC_{pH}$	0.21	100	0.21	0	0.00
	OLF_{DL}	0.10	0	0.00	100	0.10
	AREA	0.05	0	0.00	100	0.05
West Coast-Tasman-Nelson	GRP	2.45	45	2.03	55	2.80
	HYD	1.24	42	1.25	58	1.23
	LUI	0.77	100	0.77	0	0.00
	NBP	0.37	47	0.10	53	0.60
	HYD_{DL}	0.19	100	0.19	0	0.00
	OLF	0.08	0	0.00	100	0.08
	SRP	0.04	0	0.00	100	0.04
Marlborough-Canterbury	18O	0.50	100	0.50	0	0.00
	LUI	0.47	100	0.47	0	0.00
	RCD	0.21	100	0.21	0	0.00
	GANC	0.17	0	0.00	100	0.17
Southland - Otago	18O	0.68	100	0.68	0	0.00
	BGC	0.31	0	0.00	100	0.31
	OLF	0.21	0	0.00	100	0.21
	ART	0.18	100	0.18	0	0.00
	LUI	0.16	100	0.16	0	0.00
	DD	0.15	100	0.15	0	0.00
	AREA	0.07	100	0.07	0	0.00
	OLF_{DL}	0.03	100	0.03	0	0.00

Table S5.2 Nitrate-nitrite nitrogen model sensitivities by regional subset.

Region	Variable	Sensitivity	% Positive	Positive Magnitude	% Negative	Negative Magnitude
Northland - Auckland	LUI	0.96	100	0.96	0	0.00
	GRP	0.41	0	0.00	100	0.41
	GANC	0.14	0	0.00	100	0.14
	18O	0.10	0	0.00	100	0.10
	AREA	0.09	100	0.09	0	0.00
Waikato – Bay of Plenty	LUI	0.51	100	0.51	0	0.00
	RCD	0.35	100	0.35	0	0.00
	NBP	0.10	48	0.01	52	0.19
	PPT	0.08	100	0.08	0	0.00
	18O	0.06	100	0.06	0	0.00
	GTH	0.05	100	0.05	0	0.00
	HYD_{DL}	0.03	100	0.03	0	0.00
	OLF_{DL}	0.01	100	0.01	0	0.00
Wellington-Manawatu-Taranaki	GANC	0.71	0	0.00	100	0.71
	LUI	0.65	100	0.65	0	0.00
	SRP	0.44	28	0.29	72	0.49
	$SANC_{pH}$	0.22	100	0.22	0	0.00
	HYD_{DL}	0.21	100	0.21	0	0.00
Hawkes Bay - Gisborne	$SANC_{CEC}$	0.78	100	0.78	0	0.00
	LUI	0.72	100	0.72	0	0.00
	RCD	0.49	100	0.49	0	0.00
	BGC	0.35	100	0.35	0	0.00
	18O	0.27	0	0.00	100	0.27
	DD	0.25	100	0.25	0	0.00
	NBP	0.18	0	0.00	100	0.18
West Coast-Tasman-Nelson	LUI	8.21	95	7.27	5	26.37
	ART	2.83	14	18.51	86	0.37
	OLF_{DL}	0.74	87	0.78	13	0.44
	OLF	0.18	0	0.00	100	0.18
	18O	0.12	0	0.00	100	0.12
	DD	0.12	0	0.00	100	0.12
Marlborough-Canterbury	18O	0.68	98	0.70	2	0.07
	LUI	0.59	100	0.59	0	0.00
	GANC	0.31	0	0.00	100	0.31
	PPT	0.25	96	0.26	4	0.01
	SRP	0.19	92	0.21	8	0.03
	DD	0.10	100	0.10	0	0.00
	AREA	0.00	0	0.00	100	0.00
Southland - Otago	18O	0.88	100	0.88	0	0.00
	DD	0.43	100	0.43	0	0.00
	SRP	0.34	100	0.34	0	0.00
	NBP	0.24	100	0.24	0	0.00
	LUI	0.22	100	0.22	0	0.00
	HYD	0.21	0	0.00	100	0.21
	RCD	0.19	0	0.00	100	0.19
	PPT	0.16	100	0.16	0	0.00
	BGC	0.15	0	0.00	100	0.15

Table S5.3 Total phosphorus model sensitivities by regional subset.

Region	Variable	Sensitivity	% Positive	Positive Magnitude	% Negative	Negative Magnitude
Northland - Auckland	ART	3.14	68	3.48	32	2.40
	DD	0.91	100	0.91	0	0.00
	$SANC_{CEC}$	0.46	100	0.46	0	0.00
	GRP	0.13	0	0.00	100	0.13
	NBP	0.01	0	0.00	100	0.01
Waikato – Bay of Plenty	GTH	0.68	100	0.68	0	0.00
	PPT	0.24	0	0.00	100	0.24
	18O	0.22	98	0.23	2	0.02
	HYD_{DL}	0.22	100	0.22	0	0.00
	$SANC_{pH}$	0.21	100	0.21	0	0.00
	GANC	0.16	0	0.00	100	0.16
	ART	0.14	100	0.14	0	0.00
	SGC	0.14	100	0.14	0	0.00
Wellington - Manawatu - Taranaki	O18	0.51	100	0.51	0	0.00
	PPT	0.43	0	0.00	100	0.43
	EWT	0.33	0	0.00	100	0.33
	BGC	0.18	0	0.00	100	0.18
	GRP	0.06	100	0.06	0	0.00
	DD	0.02	100	0.02	0	0.00
	LUM	0.01	0	0.00	100	0.01
Hawkes Bay - Gisborne	SRP	0.98	0	0.00	100	0.98
	ART	0.67	100	0.67	0	0.00
	18O	0.66	100	0.66	0	0.00
	PPT	0.49	0	0.00	100	0.49
	HYD	0.43	100	0.43	0	0.00
	GANC	0.28	100	0.28	0	0.00
	RCD	0.24	100	0.24	0	0.00
	NBP	0.07	0	0.00	100	0.07
West Coast - Tasman - Nelson	GRP	0.87	100	0.87	0	0.00
	AREA	0.54	0	0.00	100	0.54
	ART	0.39	100	0.39	0	0.00
	HYD_{DL}	0.29	100	0.29	0	0.00
	OLF	0.27	100	0.27	0	0.00
	RCD	0.23	100	0.23	0	0.00
	GANC	0.20	100	0.20	0	0.00
	$SANC_{CEC}$	0.15	100	0.15	0	0.00
Marlborough - Canterbury	ART	1.24	0	0.00	100	1.24
	SRP	1.12	100	1.12	0	0.00
	AREA	0.44	0	0.00	100	0.44
	LUI	0.41	100	0.41	0	0.00
	BGC	0.31	0	0.00	100	0.31
	NBP	0.24	96	0.25	4	0.01
Southland - Otago	ART	0.35	100	0.35	0	0.00
	LUM	0.32	100	0.32	0	0.00
	18O	0.27	74	0.28	26	0.22
	GANC	0.25	0	0.00	100	0.25
	OLF	0.20	0	0.00	100	0.20
	BGC	0.12	100	0.12	0	0.00

ESSOAr | https://doi.org/10.1002/essoar.10507536.1 | CC_BY_4.0 | This content has not been peer reviewed.

Table S5.4 Dissolved reactive phosphorus model sensitivities by regional subset.

Region	Variable	Sensitivity	% Positive	Positive Magnitude	% Negative	Negative Magnitude
Northland - Auckland	ART	1.23	74	1.41	26	0.71
	EWT	0.24	100	0.24	0	0.00
	SRP	0.12	0	0.00	100	0.12
Waikato – Bay of Plenty	GTH	0.68	100	0.68	0	0.00
	RCD	0.64	100	0.64	0	0.00
	PPT	0.48	0	0.00	100	0.48
	EWT	0.38	0	0.00	100	0.38
	OLF_{DL}	0.27	100	0.27	0	0.00
	$SANC_{CEC}$	0.05	100	0.05	0	0.00
Wellington - Manawatu - Taranaki	RCD	1.11	100	1.11	0	0.00
	PPT	0.44	24	0.14	76	0.54
	EWT	0.31	0	0.00	100	0.31
	SRP	0.10	88	0.10	12	0.13
	$SANC_{CEC}$	0.09	85	0.09	15	0.08
	NBP	0.00	51	0.00	49	0.01
Hawkes Bay - Gisborne	DD	0.66	100	0.66	0	0.00
	PPT	0.57	5	0.12	95	0.59
	$SANC_{CEC}$	0.46	100	0.46	0	0.00
	GANC	0.45	100	0.45	0	0.00
	RCD	0.31	100	0.31	0	0.00
	HYD	0.21	100	0.21	0	0.00
	18O	0.14	100	0.14	0	0.00
West Coast - Tasman - Nelson	AREA	0.74	0	0.00	100	0.74
	OLF_{DL}	0.27	100	0.27	0	0.00
	PPT	0.24	2	0.03	98	0.25
	LUI	0.24	100	0.24	0	0.00
	CEC	0.22	100	0.22	0	0.00
	HYD	0.07	100	0.07	0	0.00
	RCD	0.06	0	0.00	100	0.06
	OLF	0.04	100	0.04	0	0.00
Marlborough - Canterbury	18O	0.42	100	0.42	0	0.00
	SRP	0.38	100	0.38	0	0.00
	AREA	0.21	0	0.00	100	0.21
	PPT	0.20	0	0.00	100	0.20
	GANC	0.19	100	0.19	0	0.00
	RCD	0.19	0	0.00	100	0.19
	DD	0.15	0	0.00	100	0.15
Southland - Otago	ART	0.43	93	0.45	7	0.18
	LUI	0.43	100	0.43	0	0.00
	GRP	0.25	100	0.25	0	0.00
	HYD_{DL}	0.24	96	0.25	4	0.07
	RCD	0.22	44	0.09	56	0.17
	18O	0.13	100	0.13	0	0.00
	SGC	0.08	100	0.08	0	0.00

ESSOAr | https://doi.org/10.1002/essoar.10507536.1 | CC_BY_4.0 | This content has not been peer reviewed.

Table S5.5 Turbidity model sensitivities by regional subset.

Region	Variable	Sensitivity	% Positive	Positive Magnitude	% Negative	Negative Magnitude
Northland - Auckland	SGC	0.50	0	0.00	100	0.50
	AREA	0.45	100	0.45	0	0.00
	ART	0.44	100	0.44	0	0.00
	LUM	0.39	0	0.00	100	0.39
	RCD	0.20	44	0.13	56	0.26
Waikato – Bay of Plenty	$SANC_{CEC}$	1.79	88	1.77	12	1.95
	ART	1.01	100	1.01	0	0.00
	SGC	0.72	2	17.74	98	0.39
	OLF_{DL}	0.64	89	0.54	11	1.40
	DD	0.30	100	0.30	0	0.00
	HYD	0.15	0	0.00	100	0.15
	LUI	0.05	100	0.05	0	0.00
Wellington - Manawatu - Taranaki	AREA	0.59	98	0.59	2	0.44
	18O	0.37	100	0.37	0	0.00
	PPT	0.35	0	0.00	100	0.35
	BGC	0.28	0	0.00	100	0.28
	LUM	0.22	21	0.05	79	0.27
Hawkes Bay - Gisborne	$SANC_{CEC}$	0.89	0	0.00	100	0.89
	RCD	0.68	0	0.00	100	0.68
	EWT	0.67	100	0.67	0	0.00
	GRP	0.45	62	0.49	38	0.38
	OLF_{DL}	0.44	100	0.44	0	0.00
	$SANC_{pH}$	0.34	100	0.34	0	0.00
	AREA	0.20	100	0.20	0	0.00
West Coast - Tasman - Nelson	OLF	4.07	62	3.29	38	5.34
	OLF_{DL}	0.62	84	0.61	16	0.66
	GRP	0.45	100	0.45	0	0.00
	AREA	0.37	0	0.00	100	0.37
	SRP	0.35	100	0.35	0	0.00
	LUM	0.17	0	0.00	100	0.17
Marlborough - Canterbury	LUI	0.61	100	0.61	0	0.00
	AREA	0.59	18	0.36	82	0.65
	OLF	0.49	86	0.52	14	0.25
	$SANC_{CEC}$	0.42	100	0.42	0	0.00
	OLF_{DL}	0.22	2	0.09	98	0.23
	LUM	0.15	0	0.00	100	0.15
Southland - Otago	18O	0.42	100	0.42	0	0.00
	OLF_{DL}	0.32	48	0.07	52	0.55
	HYD	0.27	100	0.27	0	0.00
	LUM	0.24	100	0.24	0	0.00
	GANC	0.23	0	0.00	100	0.23
	OLF	0.18	0	0.00	100	0.18
	$SANC_{CEC}$	0.08	100	0.08	0	0.00
	PPT	0.04	100	0.04	0	0.00

Table S5.6 Clarity (Black disk) model sensitivities by regional subset.

Region	Variable	Sensitivity	% Positive	Positive Magnitude	% Negative	Negative Magnitude
Northland - Auckland	SGC	1.39	100	1.39	0	0.00
	AREA	0.45	0	0.00	100	0.45
	GANC	0.33	0	0.00	100	0.33
	LUI	0.26	100	0.26	0	0.00
	HYD	0.26	100	0.26	0	0.00
	OLF_{DL}	0.22	0	0.00	100	0.22
	BGC	0.13	0	0.00	100	0.13
	LUM	0.13	100	0.13	0	0.00
Waikato - BOP	ART	0.96	0	0.00	100	0.96
	OLF_{DL}	0.34	0	0.00	100%	0.34
	SGC	0.34	100	0.34	0%	0.00
	O18	0.05	39	0.04	61%	0.05
	SRP	0.02	100	0.02	0%	0.00
	PPT	0.01	100	0.01	0%	0.00
	EWT	0.01	100	0.01	0%	0.00
Wellington - Manawatu - Taranaki	AREA	0.70	17	0.29	83	0.78
	18O	0.38	0	0.00	100	0.38
	BGC	0.35	53	0.36	47	0.34
	$SANC_{pH}$	0.31	0	0.00	100	0.31
Hawkes Bay - Gisborne	18O	1.40	0	0.00	100	1.40
	EWT	1.14	0	0.00	100	1.14
	$SANC_{CEC}$	0.77	100	0.77	0	0.00
	PPT	0.76	19	0.41	81	0.85
	DD	0.51	0	0.00	100	0.51
	RCD	0.44	100	0.44	0	0.00
	LUM	0.12	0	0.00	100	0.12
	OLF_{DL}	0.00	0	0.00	100	0.00
West Coast - Tasman - Nelson	GRP	0.47	0	0.00	100	0.47
	RCD	0.44	0	0.00	100	0.44
	SRP	0.30	0	0.00	100	0.30
	OLF_{DL}	0.26	0	0.00	100	0.26
	$SANC_{CEC}$	0.26	0	0.00	100	0.26
	OLF	0.21	0	0.00	100	0.21
	AREA	0.13	100	0.13	0	0.00
Marlborough - Canterbury	18O	0.60	91	0.56	9	1.02
	AREA	0.55	100	0.55	0	0.00
	HYD	0.52	0	0.00	100	0.52
	OLF_{DL}	0.47	95	0.47	5	0.40
	$SANC_{CEC}$	0.37	0	0.00	100	0.37
	PPT	0.31	0	0.00	100	0.31
	OLF	0.25	0	0.00	100	0.25
Southland - Otago	18O	0.73	0	0.00	100	0.73
	GANC	0.43	96	0.45	4	0.03
	LUM	0.27	0	0.00	100	0.27
	PPT	0.26	0	0.00	100	0.26
	HYD_{DL}	0.24	0	0.00	100	0.24
	BGC	0.22	0	0.00	100	0.22

Table S5.7 *E.coli* model sensitivities by regional subset.

Region	Variable	Sensitivity	% Positive	Positive Magnitude	% Negative	Negative Magnitude
Northland - Auckland	DD	1.65	0	0.00	100	1.65
	SRP	0.76	100	0.76	0	0.00
	LUI	0.68	100	0.68	0	0.00
	NBP	0.36	100	0.36	0	0.00
	AREA	0.34	0	0.00	100	0.34
	ART	0.27	100	0.27	0	0.00
	OLF_{DL}	0.17	100	0.17	0	0.00
	OLF	0.06	0	0.00	100	0.06
	$SANC_{CEC}$	0.05	17	0.01	83	0.06
Waikato – Bay of Plenty	ART	0.74	100	0.74	0	0.00
	LUI	0.47	100	0.47	0	0.00
	18O	0.44	100	0.44	0	0.00
	OLF_{DL}	0.12	96	0.12	4	0.04
	PPT	0.11	100	0.11	0	0.00
Wellington - Manawatu - Taranaki	ART	0.74	100	0.74	0	0.00
	LUI	0.47	100	0.47	0	0.00
	18O	0.44	100	0.44	0	0.00
	OLF_{DL}	0.12	96	0.12	4	0.04
	PPT	0.11	100	0.11	0	0.00
Hawkes Bay - Gisborne	18O	0.47	100	0.47	0	0.00
	LUI	0.40	100	0.40	0	0.00
	LUM	0.27	0	0.00	100	0.27
	PPT	0.25	0	0.00	100	0.25
	AREA	0.21	0	0.00	100	0.21
	RCD	0.20	100	0.20	0	0.00
	HYD_{DL}	0.13	100	0.13	0	0.00
West Coast-Tasman - Nelson	18O	0.97	100	0.97	0	0.00
	ART	0.86	0	0.00	100	0.86
	HYD	0.52	0	0.00	100	0.52
	LUI	0.50	100	0.50	0	0.00
	PPT	0.36	0	0.00	100	0.36
	$SANC_{CEC}$	0.32	0	0.00	100	0.32
	EWT	0.25	100	0.25	0	0.00
	RCD	0.13	0	0.00	100	0.13
Marlborough - Canterbury	ART	0.94	0	0.00	100	0.94
	LUI	0.78	100	0.78	0	0.00
	HYD_{DL}	0.64	100	0.64	0	0.00
	SRP	0.63	100	0.63	0	0.00
	OLF_{DL}	0.48	0	0.00	100	0.48
	NBP	0.41	100	0.41	0	0.00
	AREA	0.31	0	0.00	100	0.31
	PPT	0.30	100	0.30	0	0.00
Southland - Otago	18O	0.86	100	0.86	0	0.00
	ART	0.51	100	0.51	0	0.00
	LUM	0.45	100	0.45	0	0.00
	SGC	0.21	100	0.21	0	0.00
	$SANC_{CEC}$	0.07	100	0.07	0	0.00
	PPT	0.06	100	0.06	0	0.00